Universidade de Aveiro

Ano 2021

Departamento de Engenharia de Materiais e Cerâmica

Luís Pedro Vieira Alexandrino

Nanofibras por eletrofiação de ε-policaprolactona (PCL) e produtos naturais para aplicações dentárias

Electrospun nanofibers of ε-polycaprolactone (PCL) and natural products for dental applications

Universidade de Aveiro

Ano 2021

Departamento de Engenharia de Materiais e Cerâmica

Luís Pedro Vieira Alexandrino

Nanofibras por eletrofiação de ε-policaprolactona (PCL) e produtos naturais para aplicações dentárias

Electrospun nanofibers of ε-polycaprolactone (PCL) and natural products for dental applications

Dissertação apresentada à Universidade de Aveiro para cumprimento dos requisitos necessários à obtenção do grau de Mestre em Materiais e Dispositivos Biomédicos, realizada sob a orientação científica da Doutora Maria Helena Figueira Vaz Fernandes, Professora Associada do Departamento de Eng.ª de Materiais e Cerâmica da Universidade de Aveiro e co-orientação da Doutora Maria Ascensão Ferreira Silva Lopes | Professora Associada com Agregação da Faculdade de Engenharia da Universidade do Porto e do Doutor José Domingos da Silva Santos, Professor Associado com Agregação da Faculdade de Engenharia da Universidade do Porto

Em todo o início há um fim e nesse fim começa o início de tudo.

o júri

Presidente

Prof. Doutor João André da Costa Tedim
Professor assistente da Universidade de Aveiro

Prof.ª Doutora Maria Helena Figueira Vaz Fernandes
Professora associada da Universidade de Aveiro

Doutora Paula Alexandrina de Aguiar Pereira Marques
Investigadora da Universidade de Aveiro

agradecimentos

No desenvolvimento deste trabalho quero agradecer em especial a todas as pessoas que me acompanharam, aos meus pais, aos meus amigos e colegas. Aquelas pessoas que me animaram, acompanharam e aturaram ao longo deste percurso e durante todo o meu percurso académico e pessoal.

Quero também agradecer a todas as pessoas do laboratório, à Eng.ª. Marta Ferro pela sua ajuda e disponibilidade no SEM. Ao prof. Alexandre e à Doutora Érika Davim pela ajuda nos ensaios condutividade e de viscosidade. À Doutora Cristina Neves pela sua disponibilidade e ajuda nas medições do ângulo de contacto. À prof.ª Sandra Vieira e à Sónia Ferreira do departamento de Ciências Médicas que me ajudaram na avaliação da atividade antibacteriana.

E, por fim, aos meus orientadores Prof.ª Maria Helena, Prof.ª Maria Ascensão e Prof. José Domingos pelo apoio e sugestões que me deram ao longo do desenvolvimento neste trabalho.

palavras-chave

eletrofiação, tecido periodontal, policaprolactona, curcumina, aloé vera, eletronetting, nano-net, nanofibras, scaffold, testes antibacterianos

resumo

A doença periodontal, ou periodontite, é um problema de que muitas pessoas sofrem e não existe um tratamento que elimine eficazmente o problema. A periodontite é uma doença que provoca o colapso da estrutura periodontal, levando à necessidade de criação de estruturas capazes de facilitar a regeneração do tecido danificado.

Nesta dissertação de mestrado a abordagem para ultrapassar o problema foi fabricar membranas fibrosas através da técnica de eletrofiação, para mimetizar a matriz extracelular, usando poli(caprolactona) (PCL) à qual se adicionaram produtos naturais, como aloé vera (AV) e curcumina (CUR) para fornecer um efeito antibacteriano, e recorrendo a solventes não tóxicos, como os ácidos acético e fórmico.

As membranas eletrofiadas de PCL, PCL / AV e PCL / CUR foram produzidas com sucesso, com uma gama de diâmetros de fibras de 120-180 nm, tendo-se observado, em algumas delas, a formação de nano-teias entre as fibras, atingindo diâmetros entre 25-35 nm. As fibras foram analisadas em Microscópio Eletrónico de Varrimento e a presença de curcumina e aloé vera nas fibras foi confirmada por espectroscopia de Infravermelho por transformada de Fourier em modo de reflexão total atenuada (ATR-FTIR). Testes de molhabilidade e testes antibacterianos (*E. coli* e *S. Aureus*) foram realizados em todas as membranas produzidas.

O estudo demonstrou que a curcumina e a aloé vera podem ser carregadas com sucesso em membranas de PCL sem alterar a molhabilidade da membrana. O método de difusão em disco, que quantifica os diâmetros dos halos de inibição, não permitiu identificar atividade antibacteriana quer da curcumina quer da aloé vera.

No geral, foram produzidas com sucesso membranas de PCL, de PCL/AV e de PCL/CUR com diferentes concentrações de produto natural, com microestruturas mimetizando, à escala nanométrica, as matrizes extracelulares encontradas na estrutura periodontal. Sob o ponto de vista morfológico estas membranas apresentam-se como promissores *scaffolds* para engenharia de tecidos. A possibilidade de controlar a produção das nano-teias e o estudo mais sistemático da atividade antibacteriana destas membranas surgem assim como vertentes de grande interesse para a continuação do trabalho desenvolvido.

keywords

electrospinning, periodontal tissue, poly(caprolactone), curcumin, aloe vera, electronetting, nanofibers, scaffold

abstract

Periodontal disease, or periodontitis, is a problem that many people suffer from, and no treatment can eliminate without any doubt the issue.
Periodontal disease causes the breakdown of periodontal structure, leading to a search on creating structures capable of facilitating periodontal tissue regeneration.
In this master's thesis, the approach to overcome the problem was to manufacture fibrous membranes through the electrospinning technique to mimic the extracellular matrix. Electrospun membranes of poly(caprolactone) (PCL) and PCL loaded with natural products such as aloe vera (AV) and curcumin (CUR), were produced, to provide an antibacterial effect, using benign solvents, as acetic and formic acids.
Electrospun membranes of PCL, PCL/AV and PCL/CUR were successfully produced, with a diameter range of fibers of 120-180 nm, having been observed in some of them, the formation of nano-nets between the fibers, reaching diameters of 25-45 nm. The fibers were analyzed using Scanning Electron Microscope (SEM). The loading of aloe vera and curcumin in the fibers was confirmed using Attenuated Total Reflectance – Fourier Transform Infrared (ATR-FTIR). Wettability tests and antibacterial assay (*E. coli* and *S. Aureus*) were performed in every produced membrane.
The study demonstrated that aloe vera and curcumin can be successfully loaded into a PCL membrane without changing the wettability of the membrane. The diffusion disks method, that quantifies the diameter of inhibition halo, it was not detected any antibacterial activity with the loading of aloe vera and curcumin.
Overall, PCL membranes loaded with the different content percentages of aloe vera and curcumin were produced successfully, with nanostructure mimicking the extracellular matrices found in the periodontal structure. From a morphological perspective, these membranes are promising scaffolds for tissue engineering. The possibility of controlling the production of nano-net and a more systematic study of these membranes' antibacterial activity thus appears as aspects of great interest for the continuation of the work developed.

Index

Figure Index ..... **vi**

Table index ..... **ix**

Abbreviations ..... **x**

1. Literature Review **1**

1.1. PERIODONTAL DISEASE **1**

1.2. GUIDED TISSUE REGENERATION AND GUIDED BONE REGENERATION **2**

1.3. PCL MEMBRANES **4**

1.4. NATURAL PRODUCTS **5**

1.4.1. CURCUMIN 5

1.4.2. ALOE VERA 6

1.4.3. ANTIBACTERIAL ACTIVITY 8

1.5. ELECTROSPINNING PROCESS **9**

1.5.1. SOLUTION PARAMETERS 12

1.5.2. PROCESSING PARAMETERS 13

1.5.3. AMBIENTAL PARAMETERS 15

1.6. SOLVENTS USED FOR ELECTROSPINNING **15**

2. Materials and Methods **18**

2.1. MATERIALS AND REAGENTS **18**

2.2. SOLUTION PREPARATION FOR ELECTROSPINNING **18**

2.3. ELECTROSPINNING PROCEDURE AND PARAMETERS 19

2.4. CHARACTERIZATION 21

2.4.1. SCANNING ELECTRON MICROSCOPE (SEM) ANALYSIS 21

2.4.2. VISCOSITY AND CONDUCTIVITY MEASUREMENTS OF THE SOLUTION 21

2.4.3. FOURIER TRANSFORM INFRARED (FTIR) SPECTROSCOPIC MEASUREMENTS 21

2.4.4. WETTABILITY TESTS 21

2.5. ANTIBACTERIAL ACTIVITY ASSAY OF ELECTROSPUN MEMBRANES 22

2.6. STATISTICAL ANALYSIS 23

3. Results and discussion 24

3.1. ELECTROSPINNING 24

3.1.1. OPTIMIZATION OF OPERATING CONDITIONS OF NEAT PCL 24

3.1.2. SOLUTION PROPERTIES 26

3.1.3. ELECTROSPUN MEMBRANES OF PCL LOADED WITH CURCUMIN AND ALOE VERA 29

3.2. PHYSICAL CHEMICAL CHARACTERIZATION OF SCAFFOLDS 36

3.2.1. ATTENUATED TOTAL REFLECTION – FOURIER TRANSFORM INFRA-RED (ATR-FTIR) 36

3.2.2. WETTABILITY TESTS 36

3.3. ANTIBACTERIAL ACTIVITY ASSAY OF ELECTROSPUN MEMBRANES 38

4. Conclusion and future approaches 40

5. Bibliography 42

6. Appendix 52

6.1. FLOW RATE CORRECTION 52

Figure Index

FIGURE 1: PERIODONTIUM UNIT: GINGIVA, PERIODONTAL LIGAMENT (PDL), CEMENTUM AND ALVEOLAR BONE. ADAPTED IMAGE FROM [3]. 1

FIGURE 2: POLY(CAPROLACTONE) CHEMICAL STRUCTURE 4

FIGURE 3: CURCUMIN CHEMICAL STRUCTURE, $C_{21}H_{20}O_6$ 6

FIGURE 4: SCHEMATIC COMPOSITION OF ALOE VERA PLANT AND A CROSS SECTION OF ALOE VERA LEAF. ADAPTED FROM [45]. 7

FIGURE 5: STRUCTURE OF ACEMANNAN, EXTRACTED FROM *ALOE VERA*. 9

FIGURE 6: IMAGE OF JET OF GLYCINE WITH THE FORMATION OF TAYLOR CONE[59] 10

FIGURE 7: SCHEMATIC OF A TYPICAL ELECTROSPINNING EQUIPMENT. 10

FIGURE 8: REPRESENTATION OF BEADS IN PCL NANOFIBERS. **(A)** NANOFIBER WITH THE PRESENCE OF BEADS (YELLOW CIRCLES); **(B)** NANOFIBER WITHOUT THE PRESENCE OF BEADS. 11

FIGURE 9: ELECTROSPINNING EQUIPMENT (FLUIDNATEK LE-10) 19

FIGURE 10: CONTACT ANGLE MEASUREMENTS EQUIPMENT (ATTENTION® THETA BY BIOLIN SCIENTIFIC) AND ONEATTENSION SOFTWARE. 22

FIGURE 11: SAMPLE 1 OF PCL. **(A)** SEM IMAGE OF PCL **(B)** OUTPUT IMAGE AFTER THE USE OF THE PLUGIN "*ORIENATIONJ ANALYSIS*"; **(C)** HISTOGRAM OF FIBER DIAMETER FROM IMAGE A; **(D)** DISTRIBUTION OF ANGLE OF IMAGE A, USING "*ORIENTATIONJ DISTRIBUTION*". 25

FIGURE 12: VISCOSITY OF PCL AND PCL/CUR-2 SOLUTIONS AS-PREPARED AND AFTER ONE WEEK. SOLUTIONS AFTER 1 DAY STIRRING (INVERTED GREEN TRINGLE) AND 7 DAYS STIRRING (ORANGE TRINGLE) 27

FIGURE 13: VISCOSITY MEASUREMENTS OF PCL (GREY CIRCLE) AND PCL BLENDS OF AV (INVERTED GREEN TRIANGLE) AND CUR (ORANGE TRIANGLE) WITH DIFFERENT PERCENTAGES. (*P<0.05) 28

FIGURE 14: CONDUCTIVITY MEASUREMENTS OF SOLUTIONS WITH DIFFERENT PERCENTAGES OF PCL LOADED WITH ALOE VERA (LEFT AXIS, INVERTED GREEN TRIANGLE) AND CURCUMIN (RIGHT AXIS, ORANGE TRIANGLE). (*P<0.05) 29

FIGURE 15: SEM IMAGE OF PCL LOADED WITH ALOE VERA AT DIFFERENT PERCENTAGES, A COLOR IMAGE FROM SEM USING *ORIENTATION J* (BELOW), AND THEIR COHERENCY PERCENTAGE. 30

FIGURE 16: SEM IMAGE OF PCL LOADED WITH CURCUMIN AT DIFFERENT PERCENTAGES, A COLOR IMAGE FROM SEM USING *ORIENTATION J* (BELOW), AND THEIR COHERENCY PERCENTAGE. 31

FIGURE 17: SEM IMAGE OF PCL/AV-5 MEMBRANE SHOWING THE FIBER ON THE GREEN ARROW, AND AROUND THE CIRCLE THE NANO-NET FORMATION. 31

FIGURE 18: BOXPLOT OF FIBER DIAMETERS OF ELECTROSPUN MEMBRANES OF PCL, PCL/AV, AND PCL/CUR AT DIFFERENT CONTENT PERCENTAGE. GREEN BOXES REFER TO DIAMETERS OF THE MAIN MEMBRANE FIBERS AND RED BOXES TO NANO-NET FIBERS. 33

FIGURE 19: ELECTROSPUN NANOFIBERS AND NANO-WEBS SHOWN, WHERE AN APPROXIMATION OF THE RED SQUARE SECTION CAN BE SEEN INSIDE THE YELLOW SQUARES TO OBSERVE THE NANO-NETS, (A) PCL/AV-2; (B) PCL/AV-3; (C) PCL/AV-5; (D) PCL/CUR-1.....34

FIGURE 20: ATR-FTIR ANALYSIS OF PCL, PCL/AV-5, AND PCL/CUR-5 ELECTROSPUN MEMBRANES AND AV AND CUR POWDER.....36

FIGURE 21: CONTACT ANGLE ANALYSIS OF WATER DROP ON THE ELECTROSPUN PCL MEMBRANES LOADED WITH ALOE VERA (INVERTED GREEN TRIANGLE) AND WITH CURCUMIN (ORANGE TRIANGLE). (* P<0.05).....37

FIGURE 22: CORRELATION GRAPH BETWEEN THE FLOW RATE OF THE EQUIPMENT, AGAINST THE REAL FLOW RATE USING A 6ML SYRINGE, AND THE LINEAR CORRELATION. 52

Table index

TABLE 1: COMMERCIALLY AVAILABLE RESORBABLE SYNTHETIC BARRIER MEMBRANES, ADAPTED FROM [8]..... 3

TABLE 2: PARAMETERS USED FOR ELECTROSPINNING, SOLVENTS, MATERIALS, AND PURPOSE OF EACH REPORT USING PCL AND BIOACTIVE COMPOUNDS..... **ERROR! BOOKMARK NOT DEFINED.**

TABLE 3: ELECTROSPINNING PARAMETERS USED BY EZHILARASU ET AL.[16].....17

TABLE 4: SAMPLE DESIGNATION AND MASS PERCENTAGE OF NATURAL PRODUCTS USED IN THE ELECTROSPUN MEMBRANES. SOLVENT – AA:AF (1:2).....18

TABLE 5: THE REAL FLOW RATE READINGS, COMPARED TO THE FLOW RATE SET ONTO THE ELECTROSPINNING EQUIPMENT. 20

TABLE 6: OPERATIONAL PARAMETERS FOR PROCESSING PCL 20

TABLE 7: OPERATIONAL CONDITIONS OF SAMPLE 1. 26

TABLE 8: FIBER DIAMETER AND COHERENCY ALIGNMENT FOR EVERY ELECTROSPUN MEMBRANE OF PCL WITH THE BIOACTIVE COMPOUND WITH DIFFERENT %W/W. 32

TABLE 9: TESTS RESULTS OF ANTIBACTERIAL ASSAY OF PCL/CUR AND PCL/AV SAMPLES WITH DIFFERENT WT.% AGAINST *E. COLI* (ATCC 25922) AND *S. AUREUS* (ATCC 29213) 24H INCUBATION. 38

Abbreviations

AA	Acetic acid
AF	Formic acid
ATR-FTIR	Attenuated Total Reflection – Fourier Transform Infrared
AV	Aloe Vera
BNNTs	Boron nitride nanotubes
CUR	Curcumin
Cur@MSN	Curcumin incorporated in mesoporous silica nanoparticles
DCM	Dichloromethane
DMF	Dimethylformamide
ECM	Extracellular matrix
e-PTFE	Expanded poly(tetrafluoroethylene)
ESN	Electrospinning/netting
F-108	Copolymer F-108
FDA	Food and Drugs Administration
GBR	Guided Bone Regeneration
Gel	Gelatin
GTR	Guided Tissue Regeneration
HAS	Human Serum Albumin
HFIP	Hexofluoroisopropanol
HNT	Silane-modified halloysite nanotube
MHA	Mueller-Hinton agar
MMT	Montmorillonite
NCs	Chitosan nanoparticle
NFN	Nanofiber netting

PA-6	Poly(amide-6)
PA-66	Poly(amide-66)
PAA	Poly(acrylic acid)
PCL	Poly(caprolactone)
PDL	Periodontal ligament
PDLLA	Poly(DL-Lactic Acid)
PDLLA-NMP	Poly(DL-Lactic Acid)-N-methyl-2-pyrrolidone
PDLLCL	Poly(DL-lactide-ε-caprolactone)
PEG	Poly(ethylene glycol)
PEO	Poly(ethylene oxide)
PGA	Poly(glycolic acid)
PGA-TMC	Poly(glycolic acid) Trimethylene Carbonate
PLA	Poly(lactic acid)
PLDLGA_TMC	Poly(LD-lactic-glycolic acid) trimethylene carbonate
PLGA	Poly(Lactic-Glycolic Acid)
PTFE	Poly(tetrafluoroethylene)
PU	Poly(urethane)
PVA	Poly(vinyl alcohol)
ROS	Reactive Oxygen Species
SD	Standard Deviation
SEM	Scanning Electron Microscope
TCH	Tetracycline Hydrocloride
T_g	Glass transition temperature
Ti	Titanium
Ti-PTFE	Titanium-reinforced poly(tetrafluoroethylene)
T_m	Melting temperature

WHO	World Health Organization

1. Literature Review

1.1. Periodontal disease

There are several diseases where oral hygiene is the primary cause of chronic dental disease, and according to World Health Organization (WHO), dental caries and periodontal disease are among them. In Europe, severe periodontal disease can be found in 5-20% of middle-aged (35-44 years) adults and up to 40% of older people (65-74 years).[1]

Periodontal disease is in the periodontium. Periodontium is a functional unit that is composed of the gingiva, alveolar bone, periodontal ligament, and cementum.[2] (figure 1)

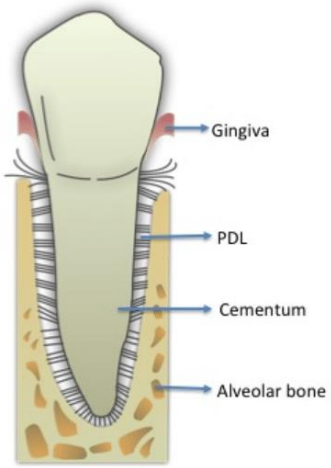

Figure 1: Periodontium unit: gingiva, periodontal ligament (PDL), cementum and alveolar bone. Adapted image from [3].

Periodontal disease, or periodontitis, causes the periodontal ligament and alveolar bone breakdown. Periodontitis treatment outcome and diagnosis vary according to disease severity and patient factors. The ideal goal is the regeneration of the reduced periodontium, meaning the regeneration of alveolar bone, periodontal ligament, and cementum, thus restoring the lost structures.[2,4]

The research field to meet the ideal goal are tissue engineering and regenerative medicine. They are a promising field that applies engineering and biological sciences

knowledge to build artifacts that promote the regeneration of tissues or organs. Strategies using biomaterials, scaffolds, and cells, and the combination of these, have been developed to stimulate the growth of lost tissue or lost functions. Several therapies have received Food and Drug Administration (FDA) approval and are commercially available.

1.2. Guided tissue regeneration and guided bone regeneration

To regenerate and repair the damaged periodontal tissues are two main surgical approaches, such as, guided tissue regeneration (GTR) and guided bone regeneration (GBR). In both guided regenerations, the use of material to prevent the growth of connective and epithelial tissues into the defect allows the regeneration of periodontal tissues.

Membranes for guided regeneration are used to support tissue regeneration, requiring specific properties that can allow the proper healing. These membranes need to be biocompatible to integrate into tissues without inducing inflammation. They also must have a degradation profile that matches the regeneration of the tissues. In the case of periodontal tissue, degradation takes typically around 4-6 weeks. Their mechanical and physical properties must be suitable for their placement *in vivo* and function as a barrier to epithelial and connective tissue growth. Since the membranes will be placed during surgery, a high resistance to tear and rupture is desirable. The membranes must also be porous to allow cellular adaption and sufficient nutrient permeation. And last but not least, they should be osteoconductive around the bone graft. A requirement of utmost importance is antibacterial activity to prevent infection of the damaged tissue.[5–7]

There are two types of periodontal membranes, non-resorbable membranes and resorbable membranes. First-generation regeneration membranes are the non-resorbable ones. The second-generation comprises natural polymer membranes, such as collagen or chitosan, and synthetic polymer membranes, such as polyesters. In the third-generation membranes, we find barrier membranes with antibacterial activity, barrier membranes with bioactive calcium phosphate incorporation, and growth factor release.[4]

Currently, there are non-resorbable membranes on the market, synthetic and natural resorbable barrier membranes. Non-resorbable barrier membranes are made of poly(tetrafluoroethylene) (PTFE), expanded PTFE (e-PTFE), titanium (Ti), and titanium-reinforced PTFE (Ti-PTFE). Still, they are not the best choice because they require a second surgery for removal. However, some surgeons continue to use these membranes because of their mechanical properties, surgical handling properties, and space maintenance for large alveolar ridge defects.

Resorbable barrier membranes can be produced using two types of materials, natural or synthetic. The most common natural materials used in these membranes are type I and type III collagen. Type I collagen is the most prevalent of the collagens present in the human body. The FDA approves type I and III collagen membranes. On the other hand, in synthetic resorbable barrier membranes, the use of poly(lactic acid) (PLA), poly(glycolic acid) (PGA), various blends of these materials are predominant, as can be seen in table 1.[8]

Table 1: Commercially available Resorbable Synthetic Barrier Membranes, adapted from [8].

Product (Company)	**Material**
Guidor® (Sunstar)	PLA
Resorb X® (XLS Martin)	PDLLA (poly(DL-Lactic acid))
Cytoflex Resorb® (Unicare Biomedical)	PLGA (poly(Lactic-Glycolic acid))
Resolute® (Gore®)	PGA-TMC (poly(glycolic acid) Trimethylene Carbonate)
Epi-Guide® (Curasan, Inc.)	PDLLA
Atrisorb (Tolmar)	PDLLA-NMP (PDLLA-N-methyl-2-pyrrolidone)
Inion™ GTR (Inion)	PLDLGA_TMC (poly(LD-lactic-glycolic acid) Trimethylene Carbonate)
Vivosorb® (Polyganics)	PDLLCL (poly(DL-lactide-ε-caprolactone))
Tisseos® (Biomedical Tissues SAS)	PLGA

For the production of periodontal membranes, different techniques are used, such as solvent casting[9], freeze-drying[10], phase separation[11], and electrospinning[12]. All of these techniques have in common the production of membranes and films creating a scaffold for tissue and bone regeneration.[13]

Presently, in the third-generation membranes, the goal is to have biodegradable materials and functionalized scaffolds to produce GTR membranes. In recent studies, membranes of a biodegradable material, such as poly(caprolactone) (PCL), have been developed and functionalized with different additives, such as nanoparticles[14], antibiotics[15], and natural products[16]. PCL has also shown that it can be used as a GTR membrane because of its good biocompatibility, proper mechanical strength, and biodegradability. It can also be manufactured via the electrospinning technique.[7]

1.3. PCL membranes

PCL is a semi-crystalline, FDA-approved linear synthetic slow-degrading aliphatic polyester (figure 2) with non-toxic products of degradation that are quickly metabolized and expelled in the human body, in the form of carboxylic acid. The degradation process of PCL in the physiological environment occurs through oxidative, enzymatic, and pH-related catalysis of hydrolysis. Small polymer fragments are entirely metabolized by cells after an initial decrease in molecular weight and subsequent macroscopic structural breakdown. PCL has a low melting temperature (~-60°C glass transition, T_g; ~60°C, melting, T_m), variable viscosity, and their degradation rate and mechanical properties can be changed when blended with other polymer and bioactive compounds.[7,16–19]

PCL is one of the most investigated polymers in the biomaterials and pharmaceutical fields. It is known because of its properties, as said before, biocompatibility, biodegradability, chemical stability, thermal stability, good mechanical properties for tissue engineering, tissue-compatible nature, permeability, and can be used as a GTR membrane. PCL can be dissolved using single solvents or a mixture of solvents. According to the literature, PCL can be dissolved using benign solvents, such as ethanol, formic acid, acetic acid, and acetone.[7,16,19]

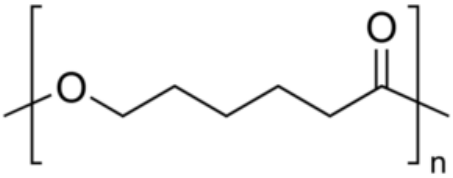

Figure 2: Poly(caprolactone) chemical structure

The drawback of neat PCL is its hydrophobic nature, which results in poor cellular response due to its lack of affinity. However, PCL can be blended with natural and synthetic polymers to overcome its poor cellular response and enhance its mechanical properties. Studies have shown that PCL can be blended with synthetic polymers, such as PLA[20], and poly(vinyl alcohol) (PVA)[21], and natural polymers, such as gelatin (Gel)[14] and chitosan[22]. PCL bioactivity and antibacterial activity can be enhanced by loading bioactive compounds of natural products, such as aloe vera and curcumin. Studies have shown that the loading of aloe vera and curcumin (CUR) on PCL nanofibers can improve cellular recognition and have antibacterial properties, which enhance cellular proliferation and adhesion and have also have an antibacterial effect incorporated in the membrane[16,23,24].

1.4. Natural products

Throughout history, the use of natural products to benefit ourselves has always been present. Medicinal plants are plants with bioactive compounds that can treat different illnesses. Natural bioactive compounds, also known as natural products, are metabolites manufactured by plants used in different fields, such as pharmaceutical drugs and bio-pesticides.

Natural bioactive compounds extracts are responsible for approximately 85% of traditional medicine preparation because they present benefits and have several advantages. They can be safe for human consumption, are associated with non-environmental pollution, present biological activity, and can develop formulations that allow the delivery of non-toxic concentrations providing at the same time an antibacterial effect. In this group, one can include the bioactive active compound curcumin, and the natural products of aloe vera present several advantages, such as anti-inflammatory effect, antibacterial and healing properties[25,26].

1.4.1. Curcumin

Curcumin is a polyphenol that is present in turmeric (*Curcuma longa L.*). Curcumin is used as a food additive, preservative, and coloring agent in Asian countries. In old Hindu medicine, it is extensively used to treat injuries. The coloring principle of curcumin is the main component of this plant, and it is responsible for its biological activity.

Curcumin and two other derivative compounds, bisdemethoxycurcumin, and desmethoxycurcumin are present in turmeric, but curcumin is the most abundant curcuminoid, figure 3. Curcumin is a yellow crystalline compound belonging to the flavonoid group. It is almost insoluble in acidic or neutral pH water, but it is soluble in strong acidic solvents, such as glacial acetic acid and polar or non-polar solvents. It has a melting point of 183°C, and its molecular weight is 368,38 mol/g.

Clinical studies show that curcumin is considered safe for human consumption, even at high doses. It presents several benefits, including anti-inflammatory[27], anti-viral[28], antibacterial[29], anti-carcinogenic[30], wound healing[31], among other properties. But its medical application is extremely poor because of its bioavailability[32–34].

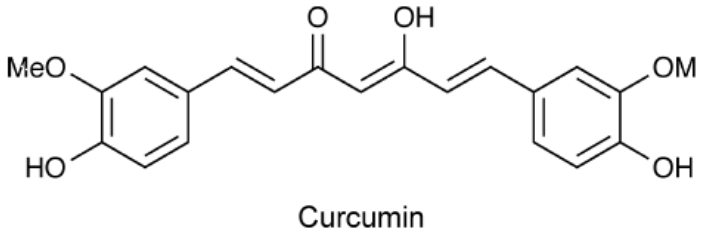

Figure 3: Curcumin chemical structure, $C_{21}H_{20}O_6$

Curcumin has been gaining interest because of its biological properties and possible loading in membrane blends improving cell proliferation and growth as a bioactive compound. Recent reports found that curcumin can be blended with PCL in the production of nanofibers membrane, using the electrospinning technique. Curcumin can be used in a drug delivery system[32,35–37] and wound healing membrane[36,38,39].

1.4.2. Aloe Vera

Aloe Vera is a medicinal plant known as *Aloe barbadensis*, used because of its beneficial properties to treat burns, wound healing, reduction of fever, among others. Aloe vera finds its origin in South and East Africa and Mediterranean regions. It is one of the most potent, commercially important, and the most popular plant in research fields.

Aloe vera is well known for its antioxidant, anti-inflammatory, anticarcinogenic, antibacterial, among other properties. Aloe vera leaves are known to have as many

as 75 nutrients and 200 bioactive compounds, including vitamins, enzymes, minerals, sugars, anthraquinones, sterols, salicylic acids, and amino acids.

Aloe vera powders can be produced via freeze-drying. It is known that aloe vera's antibacterial properties come from two sugars, called glucomannan and acemannan. These sugars also proved to accelerate wound healing, activate macrophages, stimulate the immune system, and have antiviral effects[40–42].

Aloe vera leaves are composed of three distinct layers (figure 4):

Inner layer – where aloe vera gel is found, it is soft, clear, moist, and slippery tissues that have large parenchyma cells. This is a transparent mucilaginous jelly-like material. It is composed of water (99%), glucomannans, amino acids, lipids, sterols, and vitamins[40,43].

Middle layer – called latex, composed of anthraquinones, a bitter yellow sap, and glycosides[40,43].

Outer layer – the rind, composed of 15-20 cells that protect the gel matrix and help synthesize carbohydrates and proteins[40,44].

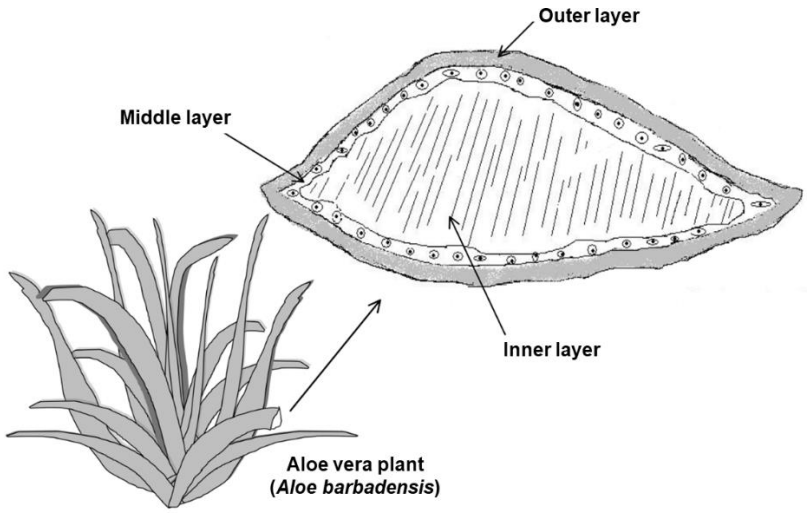

Figure 4: Schematic composition of aloe vera plant and a cross-section of aloe vera leaf. Adapted from [45].

In recent years, the use of aloe vera in tissue engineering has been developed, mainly because it was observed that aloe vera could increase the collagen content of

the tissues as well as its degree of crosslinking. Aloe vera can also stimulate fibroblasts for regeneration, enhance tensile strength, and glucomannan and gibberellin, a hormone, interact with growth factor receptors on fibroblast, therefore stimulating its activity and proliferation. Several glycoproteins present in the aloe vera have been reported to increase the proliferation of normal human dermal cells. This stimulatory on dental cells could potentially lead to an improved outcome on therapies for periodontal tissues[25,41].

Recently, aloe vera has been used in electrospinning membranes and films in blends of PCL and other synthetic polymers for skin healing[21,46,47] and drug delivery[47]. The incorporation of aloe vera in a blend of PCL and Gel showed that aloe vera enhances the proliferation of fibroblasts, exhibits antibacterial activity, and biodegradability[47].

1.4.3. Antibacterial Activity

Antibacterial activity is one of the main goals to achieve it on a GTR/GBR membrane for periodontal disease. Since the main problem with periodontitis is the development of infections, such as bacterial and viruses, a membrane with antibacterial activity could be a sensible alternative approach to treat this problem.

Periodontitis is a disease with an infectious etiology by inflammation of the supporting tissues. If not adequately treated can lead to the destruction of the periodontium and, in the long term, tooth loss. The presence of periodontopathogenic bacteria is the main reason for an increase in periodontal damage in the host. These bacteria are known to be predominantly gram-positive, such as, *Staphylococcus Aureus*, and gram-negative, such as, *Actinobacillus actinomycetemcomitans* and *Porphyromonas gingivalis*, which are known to produce multiple factors leading to tissue damage found in periodontittis[48–50].

There are two general classes of bacterial cell walls, gram-positive and gram-negative cell walls, first introduced by Hans Cristian Gram based on their different retention of crystal-violet dye. Gram-positive cell walls are thick, multi-layered peptidoglycan sheaths and, gram-negative cell walls have an outer membrane that surrounds a thin peptidoglycan layer, with a periplasmic space between the inner and outer membrane[51].

Aloe vera and curcumin are known to have antibacterial properties. Curcumin is a bioactive compound, while aloe vera is an extract. Aloe vera extract contains potentially 75 active constituents, among which there are acetylated polysaccharides, such as acemannan and (β-(1, 4)-acetylated polymannose), figure 5. Acemannan is responsible for the antibacterial activity of aloe vera, suggesting that it may block bacterial binding and is the main component in aloe-vera freeze-dried powders[41,52,53].

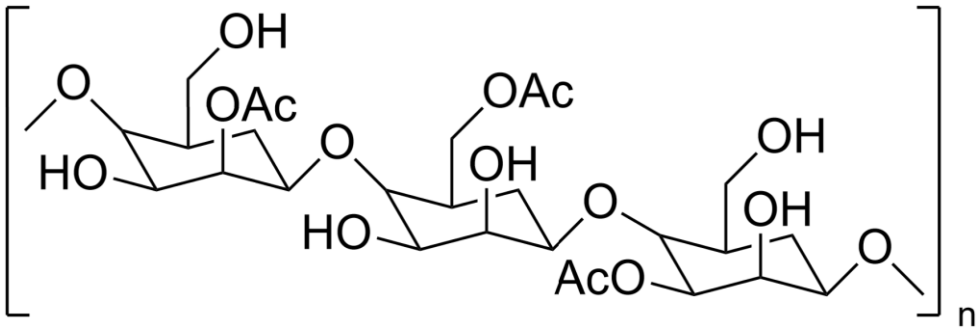

Figure 5: Structure of acemannan extracted from Aloe vera.

Studies using curcumin reported that curcumin disrupts the bacterial cell wall and proliferation, providing antibacterial activity. Curcumin is also known to be a photosensitive compound when exposed to a specific wavelength within the presence of oxygen, resulting in the production of reactive radicals, known as reactive oxygen species (ROS) that can induce cell death bacteria[52,54].

Having these properties, a membrane of PCL loaded with the different natural products, aloe vera and curcumin could be an alternative approach to treat periodontitis. GTR/GBR membranes of PCL loading aloe vera and curcumin could be developed using, for example, an electrospinning process.

1.5. Electrospinning process

The electrospinning process is gaining popularity nowadays, but it is not a new concept. The term “electrospinning” was coined in the year 1994, and it was known as “electrostatic spinning”[55] and patented by Formhals in 1934.[56,57] The fibers produced from this technique can reach diameters on the scale of micrometers and nanometers. Since then, there have been different approaches on the types of electrospinning methods, for example, melt electrospinning and electronetting[58].

In typical electrospinning equipment, a polymer solution is first fed through a spinneret, like a syringe. The nozzle of the needle acts as an electrode to which a

high voltage is applied. The high voltage is always applied to the solution at a critical voltage, typically more than 5 kV. The electrostatic forces overcome weaker surface tension forces in the charged polymer, creating the “Taylor cone” (figure 6).

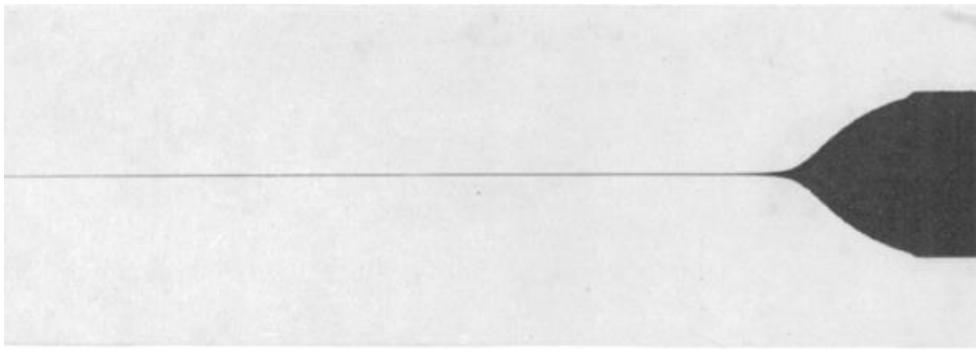

Figure 6: Image of a jet of glycine with the formation of Taylor cone[59].

As the solvent evaporates through the distance between the tip and the collector, usually 10-25 cm, the nanofibers are formed and collected in a rotating or static collector that acts as a counter electrode. Allowing the production of fine fibers with a large surface area, into a collector, as shown in figure 7. In this technique, polymer solutions or melted polymers can be used under high electric fields. Furthermore, this technique is moderately expensive, and it can be scaled up, employing multiple spinnerets.[60,61]

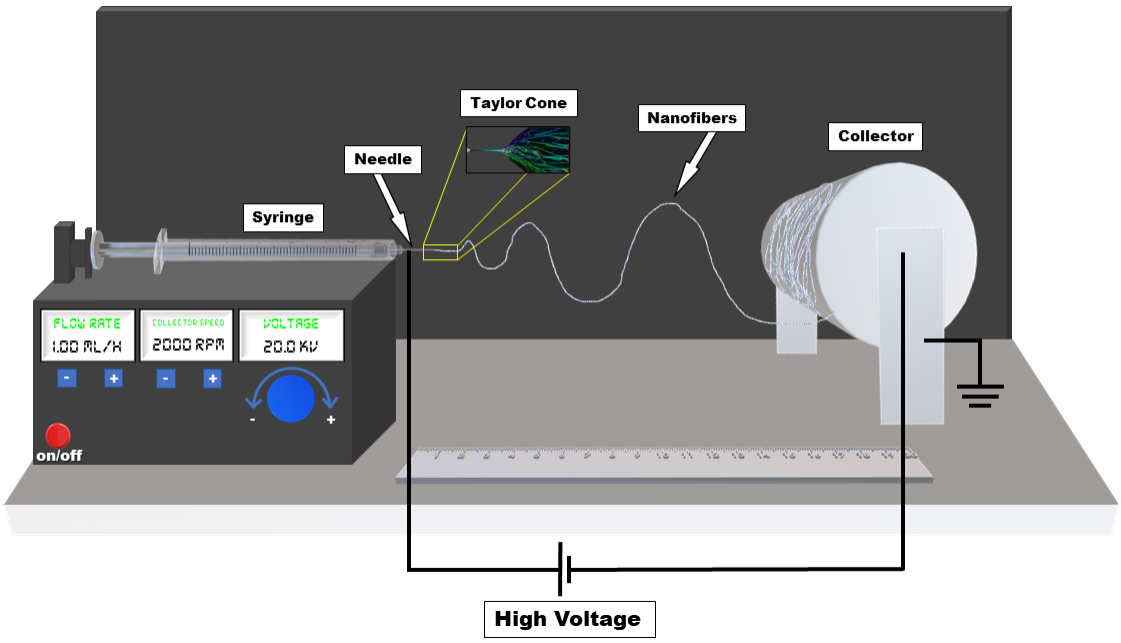

Figure 7: Schematic of typical electrospinning equipment.

Electrospun nanofibers can present undesirable beads, meaning that the solution was not subjected to electrospinning only but the electrospray process. The result looks like droplets in the fibers, as can be seen in figure 8[57,62,63].

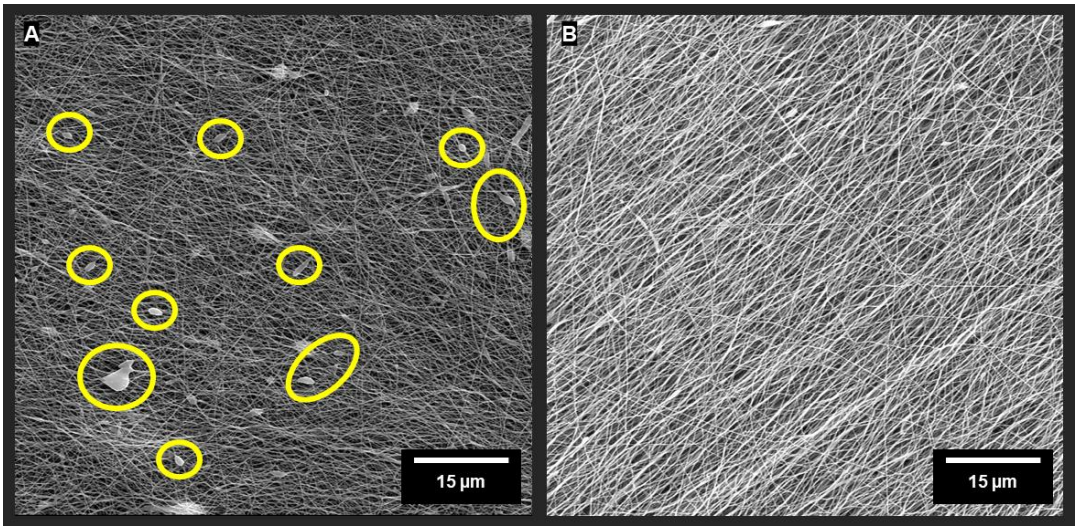

Figure 8: Representation of beads in PCL nanofibers. (A) nanofiber with the presence of beads (yellow circles); (B) nanofiber without the presence of beads.

The produced nanofibers have applicability in nanotechnology, and they can be aligned or random. These different nanofibers orientations can mimic the extracellular matrix (ECM) and should have diameters in the range of 50-500 nm[64]. ECM provides a substrate with specific ligands for cell adhesion and migration, regulates cellular proliferation and function by delivering various growth factors[65]. These biomimetic nanostructures have important implications in fundamental cell biology studies and application for regenerative medicine and medical device design[60].

The interest in the electrospinning process has increased due to producing materials with nanoscale properties. At first glance, electrospinning seems easy and very simple, but there are a lot of variables to have in mind to contribute toward the fiber morphology. Doshi and Reneker[66] divided these variables into three parameters: solution, process (controlled variables), and ambiental. The solution properties include the solution's viscosity, conductivity, and surface tension. The process parameters are the variables that can be controlled on the equipment, including hydrostatic pressure in the capillary (flow rate), the electric potential at the tip of a needle, and the distance of the needle to the collector. The Ambiental parameters include the temperature, humidity, and air velocity in the electrospinning chamber[57,66].

1.5.1. Solution parameters

The electrospinning process starts with a solution with key properties, allowing the fibers to form with the appropriate morphology, alignment, and mechanical behaviour. These key properties are the concentration, the molecular weight of the polymer used, viscosity, surface tension, and conductivity of the polymer's solution. Each property can determine the features of the final product[57,61].

Concentration

For electrospinning to have a fiber formation, a minimum solution concentration of the polymer is required. At low concentrations, fibers with a mixture of beads are obtained, and as the solution concentration increases, the shape of the beads changes from spherical to spindle-like and to finally a uniform fiber with increased diameters because of the high viscosity. Reports have shown that the polymer concentration affects the fiber diameter, where higher concentrations lead to an increase in fiber diameter. Viscosity and surface tension are essential in determining a polymer's concentration to produce continuous fibers. The higher the concentration of the solution, the higher is going to be the viscosity[61,67].

Molecular weight of the polymer

The molecular weight of the polymer interacts with beads formation. Low molecular weight solution provides a beaded fiber formation, and a high molecular weight gives fibers with a reduction of beads formation. Molecular weight interacts with the solution viscosity by the number of entanglements of polymer chains[61].

Viscosity

The solution for electrospinning needs to have an optimal viscosity, in which it can't be too low viscosity, because it will not create a continuous fiber formation, and it can't be too high viscosity, because there is going to have difficulty for the solution in the ejection of jets from polymer. It is an optimal viscosity when the ejection of jets is continuous and can produce continuous fibers. It has been reported that the maximum spinning viscosity ranges for electrospinning are 1 to 250 poise. Within this range, a lower viscosity leads to the formation of beads, and a higher one can eliminate these beads[61,68].

Surface tension

Surface tension is controlled by the composition of the solvent used in the production of the solution. A reduction of surface tension leads to smooth fibers instead of beaded fibers, and a high surface tension results in jet instability. The change in ratio solvent composition interacts with the surface tension created, and it will impact the fiber morphology[57,61].

Conductivity

The conductivity of the solution is given by the type of polymer used, the solvent composition, and the availability of ionizable salts. It has been reported that with the increase of electrical conductivity of a solution, there is a significant decrease in the diameter of electrospun nanofibers. In contrast, a low conductive solution creates an insufficient elongation of a jet by the electrical force applied to produce uniform fibers[61].

1.5.2. Processing parameters

The processing parameters, or operation parameters, are the controllable variables within the equipment to produce uniform fibers. These variables are the voltage applied, the flow rate of the solution, the type of collector, and the distance between the needle and the collector.

Applied Voltage

The voltage applied is the most essential aspect of the electrospinning, that's why the technique is called "electro". The voltage applied on electrospinning is above 5kV to induce the required amount of electrical force to form the Taylor cone and bring the solution from the tip of the needle to the collector. This process causes the beginning of the electrospinning process. Higher voltage will collect a higher amount of volume from the tip of the needle, and it can reduce the instability of the jet by shrinking the Taylor cone. Therefore if the flow rate is too low and the voltage too high, the solution can be collected faster than the flow rate. Studies have shown that a higher voltage will lead to a stretch of the solution affecting the fibers' morphology by making them thinner. The thinner they are, the faster the solvent will evaporate[61,69].

Flow rate

The flow rate influences the jet velocity and the material transfer rate. It is defined by the volume transferred in an hour. A lower flow rate is desirable because the solvent will get enough time for evaporation.[70] There should always be a minimum flow rate of the spinning solution. It is reported that the increase of flow rate leads to an increase in fiber diameter and pore diameter and results in beaded fibers due to the unavailability of proper drying time before reaching the collector[61].

Types of collectors

The electrospun fibers are collected into a collector. This collector can have different forms and shapes. Generally, they are collected to a collector plate made of aluminum sheet and are connected to the power source through a conductor to achieve a stable potential difference. But this is not the only collector available. The need for aligned fibers to various applications brought different types of collectors, such as conductive paper, conductive cloth, wire mesh, parallel or grided bar, rotating rod, rotating wheel, or to a coagulation bath with non-solvent liquid. The less conductive the collector is, the formation of beaded fibers is formed because of less surface area. Several studies have shown that using a rotating drum, wheel-like bobbin, or metal frame can be better to align the electrospun fibers, and stationary collectors can result in random electrospun fibers[57,61,69,71].

Tip to collector distance

The distance between the tip of the syringe to the collector is one important parameter in electrospinning. There is a minimum distance required because fibers need to have sufficient time to evaporate the solvent of the polymer solution between the tip of the syringe to the collector. If the distance is too close, the presence of beads on fibers can be observed because the solvent did not have the time to evaporate properly. Thus, there should be an optimum distance between the tip and collector, which favors solvent evaporation from the nanofibers[61,72].

1.5.3. Ambiental parameters

This parameter is the most difficult to control, but it's not impossible. The Ambiental parameters are the humidity, temperature, and air velocity in the electrospinning. Studies on the effect of humidity in the electrospinning process have shown that an increase in humidity leads to increased fiber diameter. Regarding the impact of temperature, it was shown that an increase in temperature (15-35°C) leads to a decrease of viscosity and increased stretching, producing thinner fiber, in some cases with the presence of beads. It is reported that ideally favourable Ambiental parameters for the electrospinning process are low humidity and temperatures between 15°C - 35°C[73].

1.6. Solvents used for electrospinning

The solvent used in the preparation of polymers solution has a significant influence on its spinnability. Organic solvents, such as chloroform[21,35–37,46], dichloromethane (DCM)[38], dimethylformamide (DMF)[21,35,38] and hexafluoroisopropanol (HFIP)[16], or a combination of these solvents, are used in electrospinning. However, they present high toxicity, making them unreliable in the biomedical field because traces of these solvents can be found on the electrospun nanofibers, presenting problems for cytocompatibility[19].

Green electrospinning has been gaining popularity these years, using benign solvents instead of the toxic known solvents. Acetic acid (AA)[32,47], formic acid (FA)[32], and distilled water are included in the group of benign solvents. Benign solvents also present advantages for the environment and present low toxicity for the human body[19,74].

To address the use of benign solvents on the production of electrospun membranes of PCL loaded with natural products, PCL could have as a solvent acetic acid and formic acid. Acetic acid can dissolve PCL pellets, but the use of formic acid increases the conductivity of the solution because of the dielectric constant, ϵ, that is higher on formic acid (ϵ = 58 at 20°C) than in acetic acid (ϵ = 6.2 at 20°C). The use of formic acid as a solvent influences electrospinning. It increases the porosity, decreases fiber diameter, and improve the distribution of fiber diameter[19,75,76].

Research using the database of Scopus, with the keywords “electrospinning PCL curcumin” and “electrospinning PCL aloe vera” since 2019 to the present, was conducted. The most recent studies using PCL with curcumin and aloe vera are shown in table 2. There was in some papers that use blends of PCL with other polymers, such as PVA[21], Gel[47], poly(ethylene oxide) (PEO)[35], montmorillonite (MMT)[38]. Table 2 summarizes the parameter used in the electrospinning process and the solvents in the polymer solutions.

Table 2: Parameters used for electrospinning, solvents, materials, and purpose of each report using PCL and bioactive compounds.

(Cur@MSN – curcumin incorporated in mesoporous silica nanoparticles[32], HNT – silane-modified halloysite nanotube[35], F-108 - copolymer F-108[36], NCs – Chitosan nanoparticle[32])

	Materials	Solvents	Voltage	Flow rate	Outcomes	References
Aloe Vera	PCL/AV	Chloroform Methanol	18 kV	10.0-15.0 mL/h	Film for skin lesions	46
	Gel/AV-PCL	Acetic Acid	15 kV	1.0 mL/h	Fibers skin substitutes	47
	PCL/PVA/ AV	DMF Chloroform	12-24 kV	1.0-3.0 mL/h	Wound healing	21
Curcumin	Cur and Cur@MSN/ PCL	Formic acid Acetic acid	20 kV	0.5 mL/h	Drug delivery system	32
	PCL/Cur	Chloroform Methanol	23 kV	1.0 mL/h	Protective clothing for targeted and controlled drug delivery	37
	PCL/PEO-Cur/HNT	DMF Chloroform	17 kV	1.0 – 1.5 mL/h	Controlled drug delivery system	35
	PCL/Cur/ F-108	Ethanol Chloroform	18 kV	0.5 mL/h	Wound healing and drug delivery system	36
	PCL/MMT/ Cur	DMF DCM	10 kV	0.3 mL/h	Wound dressing	38
	PCL/Gel/ NCs/Cur	DCM:DMF	10 kV	0.3 mL/h	Wound healing	39

Ezhilarasu et al.[16] prepared blends of PCL loaded with AV and CUR. The authors obtained electrospun nanofibers from blends of PCL/AV, PCL/Cur, PCL/AV/Cur, and PCL/AV/Tetracycline Hydrochloride (TCH), using the conditions depicted in table 3. It was found that these scaffolds possessed biocompatibility and potential use for wound dressing with the incorporation of curcumin and aloe vera. Their mechanical properties were within the range of human skin, providing an effective wound dressing

for skin tissue engineering[16]. However, the production of most of the fibers described above and presented in table 2, used toxic solvents.

Table 3: Electrospinning parameters used by Ezhilarasu et al.[16]

Material	Concentration w/v (%)	Flow rate	Voltage	Solvent
PCL	13	1.5 mL/h	14-15 kV	HFIP
PCL/AV	10:3			
PCL/CUR				
PCL/AV/CUR	9:3:1			
PCL/AV/TCH				

This work is intended to produce a resorbable barrier membrane of PCL loaded with natural products of aloe vera and curcumin, using electrospinning technique and non-toxic solvents, in this case, acetic and formic acids. The electrospun membranes are aimed to be aligned to improve cellular growth and antibacterial properties. Recent studies in our group demonstrated that it is possible to produce aligned electrospun membranes with the desired mechanical properties for GTR membranes of PCL using acetic acid and formic acid as solvents[77]. The loading of natural products in the PCL fibers is explored to develop a scaffold to act as a GTR membrane in periodontal tissue regeneration.

2. Materials and Methods

2.1. Materials and Reagents

Poly(caprolactone) (PCL, molecular weight M_n = 80 KDa, Ref. 440744), Curcumin powder from *Curcuma longa* (Turmeric), glacial acetic acid (99.8 v/v %), and formic acid (99-100 v/v %) were purchased from Sigma-Aldrich. Terra-Pure™ freeze-dried aloe vera powder 200x was purchased by Terry Laboratories LLC (Melbourne, FL UA). The chemicals/solvents were used without further purification.

2.2. Solution preparation for electrospinning

Polymer solutions loaded with different percentages of the bioactive compound were prepared. 14%(w/v) PCL solution was prepared for the neat PCL membrane. It was prepared by dissolving PCL in a mixture of acetic acid (AA) and formic acid (FA) (1:2) and stirred overnight at room temperature. The same procedure and solvents were used when loaded curcumin and aloe vera since they both are dissolved in acetic acid and formic acid.[78]

Different mass percentages of natural products were introduced in the membranes. Mass percentages of 0.5%, 1%, 2%, 3%, and 5% of natural products were added to PCL electrospun membrane, as shown in table 4.

Table 4: Sample designation and mass percentage of natural products used in the electrospun membranes. Solvent – AA:AF (1:2)

Sample	***Natural Products (wt.%)***
PCL	0
PCL/NP-0.5	0.5
PCL/NP-1	1
PCL/NP-2	2
PCL/NP-3	3
PCL/NP-5	5

2.3. Electrospinning procedure and parameters

After preparing the polymer solution, a syringe of 6 mL was used to load the solution. In this process, the syringe was then inserted into an infusion pump to which a plastic tube with a stainless-steel needle on its tip is attached, as shown in figure 9. The cylinder collector was coated with aluminum foil to simplify the collection of the electrospun membrane.

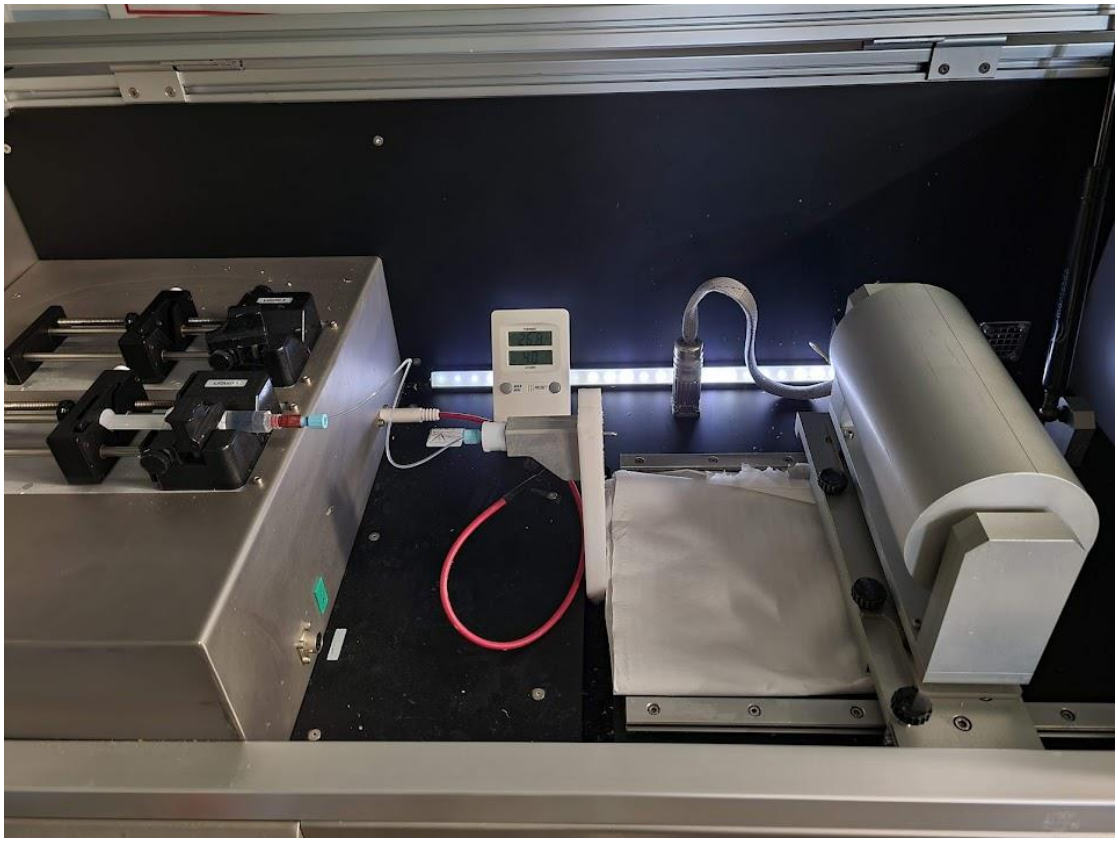

Figure 9: Electrospinning equipment (FLUIDNATEK LE-10)

The operational parameters were first optimized with neat PCL before going to the addition of the natural products. The distance of the tip of the needle to the cylinder collector and voltage was set to 18 cm and 18 kV. A study on the variation of collector speed and the flow rate was performed to produce aligned nanofibers with nanometer-scale fiber diameter.

The variation of collector speed was set from 2000 rpm to 500 rpm in different samples, and the flow rate onto the machine was 0.4 mL/h to 2.0 mL/h. The flow rate set did not correspond to the real flow rate, because a systematic error was performed. The syringe diameter was not set on the machine, leading to a default

value, 20 mm. The value of the diameter of a syringe of 6 mL, used in this work, is 1.214 cm. The real values for the flow rate are presented in table 5. From now on, the real flow rate will be called flow rate. The formulation is more detailed in appendix 1.

Table 5: Real flow rate readings compared to the flow rate set onto the electrospinning equipment.

Flow rate set (mL/h)	Real flow rate (mL/h)
0.40	0.15
1.00	0.36
1.50	0.54
2.00	0.73

The operational parameters for processing neat PCL can be found in table 6.

Table 6: Operational parameters for processing PCL

Sample	Feed rate (mL/h)	Collector velocity (rpm)	Distance (cm)	Tension (kV)	Volume (mL)	%PCL	Solvents (AA:AF)
1	0.15	2000	18	18	10	14	1:2
2	0.36						
3	0.55						
4	0.73						
5	0.15	1500					
6	0.36						
7	0.55						
8	0.73						
9	0.15	1000					
10	0.36						
11	0.55						
12	0.73						
13	0.15	500					
14	0.36						
15	0.55						
16	0.73						

After finding the best operational parameter that could produce aligned and low fiber diameter with neat PCL, the next step was loading aloe vera and curcumin separately to the solution, using the same operational parameters.

2.4. Characterization

2.4.1. Scanning electron microscope (SEM) analysis

The morphology of the nanofibers was observed using a scanning electron microscope (SEM, Hitachi S-4100, Japan). The images were taken at different magnifications and with an acceleration of 15 kV and 25 kV, depending on the type of coating. For the gold coating on the sample, the acceleration was 15 kV, and for the carbon coating, 25 kV was used.

The SEM observation on the samples of neat PCL was sputter-coated with a layer of gold, and the rest of the membranes were coated with carbon. This change was due to a problem with the gold coating equipment. The diameters of the fibers were calculated using the software ImageJ with one hundred readings of the diameter on each image on the software. The orientation analysis was obtained using Image J's plugin “OrientationJ”.

2.4.2. Viscosity and conductivity measurements of the solution

The viscosity of the polymer solutions was analysed using a Thermo ScientificTM HAAKETM viscometer. The viscosity was measured at the cut-off speed of 116 s^{-1}.

The conductivity of every polymer solution was measured with a METTLER TOLEDO Sevenmulti™.

2.4.3. Fourier transform infrared (FTIR) spectroscopic measurements

Chemical analysis of the membranes was performed via Attenuated Total Reflectance Fourier Transform Infrared (ATR-FTIR) in Bruker Tensor 27 FT-IR spectrometer (Bruker Corporation). The spectra were recorded between 4000 and 350 cm^{-1}, with a resolution of 4 cm^{-1} and 256 scans.

2.4.4. Wettability Tests

The wettability of membranes was evaluated using the Attention® Theta by Biolin Scientific equipment and analyzed using the OneAttension software, figure 10. One drop of water with a volume of ~4µL was poured on the membranes and five replicas of the process were done to each membrane.

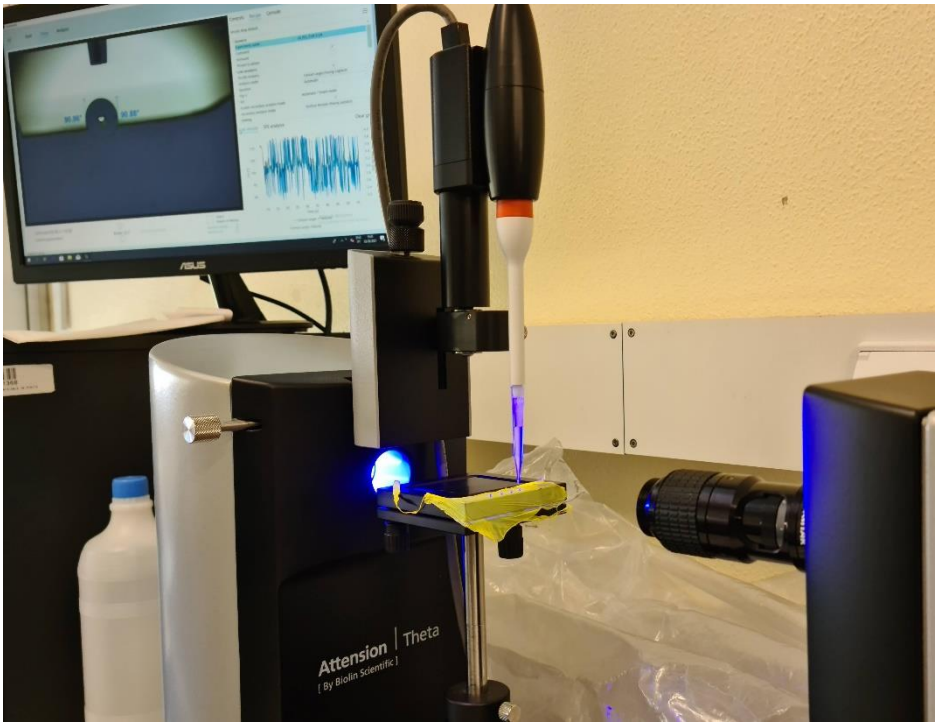

Figure 10: Contact Angle measurements equipment (Attention® Theta by Biolin Scientific) and OneAttension software.

2.5. Antibacterial activity assay of electrospun membranes

Antibacterial activity assay for the electrospun membranes with different percentages of aloe vera and curcumin was carried out using pure cell colonies of two bacterial strains: *E. Coli* (ATCC 25922) and *S. Aureus* (ATCC 25923) – using an agar diffusion method on sterile Mueller-Hinton agar (MHA) plates (BioMerieux, France). The strains were grown overnight in PVX plates (BioMerieux, France), and a suspension of 0.5 MacFarland was achieved using 0.9% NaCl saline solution. The suspension was transferred to the surface plate using a sterile swab, and all the surface was swabbed.

The electrospun membranes were cut into ~13mm disks with the aluminum foil on top and the membrane in contact with the agar surface. The agar surface with the membrane's disks was incubated for 24h at 37 °C. The control disk was the neat PCL. The antibacterial activity was determined by measuring the width of the zone of

inhibition (mm) with the repetition of three plates with each bacterial strain for PCL/CUR and PCL/AV.

2.6. Statistical analysis

Quantitative results were presented with average and standard deviation. Statistical differences were analyzed resorting to a *t-Student* distribution with a level of significance of 5% (*$p<0.05$).

The fiber diameter results were expressed as Average ± Standard Deviation (SD).

3. Results and discussion

3.1. Electrospinning

To optimize the parameters and have aligned fibers in the electrospun membranes, a study with PCL was carried out with variables of the operating conditions, such as flow rate and collector speed. The properties of solution and operation conditions, such as distance and voltage applied, were not changed from the previous study[77]. The solvents used were acetic acid and formic acid with a ratio of 1:2, and 14% PCL (w/v).

After finding the most suitable operational conditions, this means, with a higher alignment and at the same time with the adequate fiber diameter, the loading of natural products was performed, maintaining the most suitable operational parameters found for the neat PCL.

3.1.1. Optimization of operating conditions of neat PCL

In the electrospinning process, the optimal operational parameters must be found to have a range of 50-500 nm to mimic ECM. In this work, the flow rate and collector speed were tested. The distance between needle and collector and voltage applied was fixed at 18 cm and 18 kV. The room temperature was (27.0 ± 2.9) °C, and the humidity of (30 ± 1) %.

Flow rate and collector speed

Flow rates in the machine were varied between 0.15 mL/h to 0.73 mL/h, and on the collector speed, a variation of 500 to 2000 rpm was set to have the best alignment and fiber diameter.

The fibers diameters were analyzed using the software *Image J*, and the alignment of fibers with a plugin of *ImageJ* called *Orientation J*. In the plugin *OrientationJ* there is the possibility to measure the "*OrientationJ Dominant Direction*". This dominant direction has a coherency reading that goes from 0 to 1. When the coherency is 0, there is no predominant direction, therefore random alignment, but when it is close to 1, the fibers are well aligned with one of the gradient directions.

OrientationJ has a color survey that can be applied to the orientation of the fiber, called "*OrienationJ Analysis*". In figure 11B, this can be seen on the left down corner and means that in the cylindrical-coordinate color representation, the angle around the central vertical axis corresponds to hue. The higher the coherency is, the more saturated the corresponding colors are.[79]

Sample 1 of PCL was the membrane that presented a lower fiber diameter, best alignment and did not present any beads compared to the other membranes with different parameters. The analysis of sample 1 of PCL can be seen in figure 11.

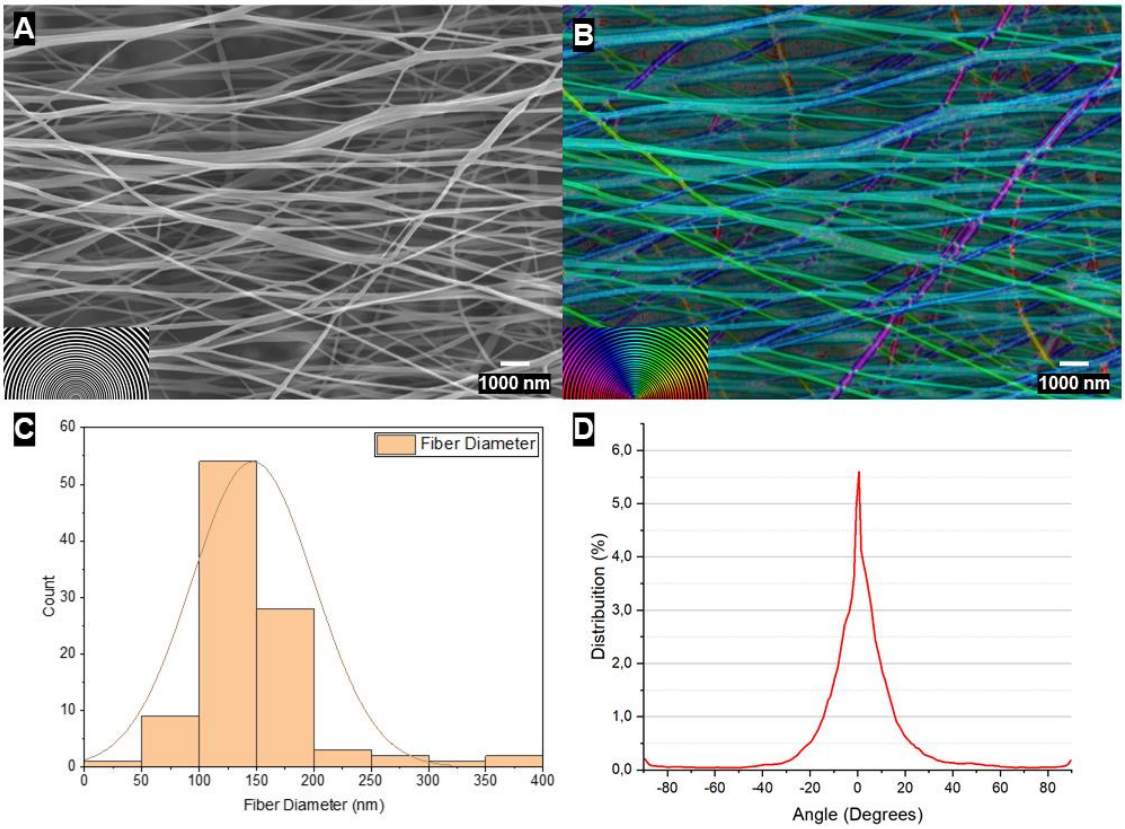

Figure 11: Sample 1 of PCL from table 6. **(A)** SEM image of PCL **(B)** Output image after the use of the plugin "*OrienationJ Analysis*"; **(C)** Histogram of fiber diameter from image A; **(D)** Distribution of angle of image A, using "*OrientationJ distribution*".

The most suitable conditions that presented a nanofiber diameter within the range of 50-500 nm and highest alignment were sample 1 with PCL with the best dominant alignment coherency (81.20%) and the lowest fiber diameter of (146.82 ± 53.38) nm. Operational conditions are described in table 7.

Table 7: Operational conditions of sample 1.

Flow rate	0.15 mL/h
Distance of needle to the collector	18 cm
Voltage	18 kV
Collector speed	2000 rpm

3.1.2. Solution properties

Viscosity

An analysis of the viscosity of the solution before electrospinning was conducted with different concentrations of curcumin and aloe vera on the solution. An exploratory study in which the viscosity of a PCL solution and PCL loaded with 2% of curcumin (PCL/CUR-2) was measured after an overnight dissolution and six days after the first measurement showed that the viscosity greatly decreased. The PCL and PCL/CUR-2 viscosity solution after an overnight stirring exhibited viscosities of respectively (405.2 ± 2.17) mPa.s and (382.2 ± 1.93) mPa.s, and, after six days the results for PCL and PCL/CUR-2 decreased to (18.3 ± 0.1) mPa.s and (14.9 ± 0.2) mPa.s, as shown in figure 12.

Based on this finding, the solutions used for electrospinning couldn't be stored but were used as prepared. The change in viscosity is attributed to PCL degradation in the acid solvent in the solution (AA:AF). It is reported in the literature that PCL degradation is strongly influenced by pH solution. The primary degradation pathway of PCL is ester hydrolysis, and acidic or basic constituents catalyze it. PCL acidic degradation consistently decreases both in molecular weight and mass and proceeds via a bulk erosion mechanism[17]. The loading of curcumin did not prevent the degradation pathway of the PCL. The viscosity of PCL obtained by overnight dissolution was in accordance with the literature[80].

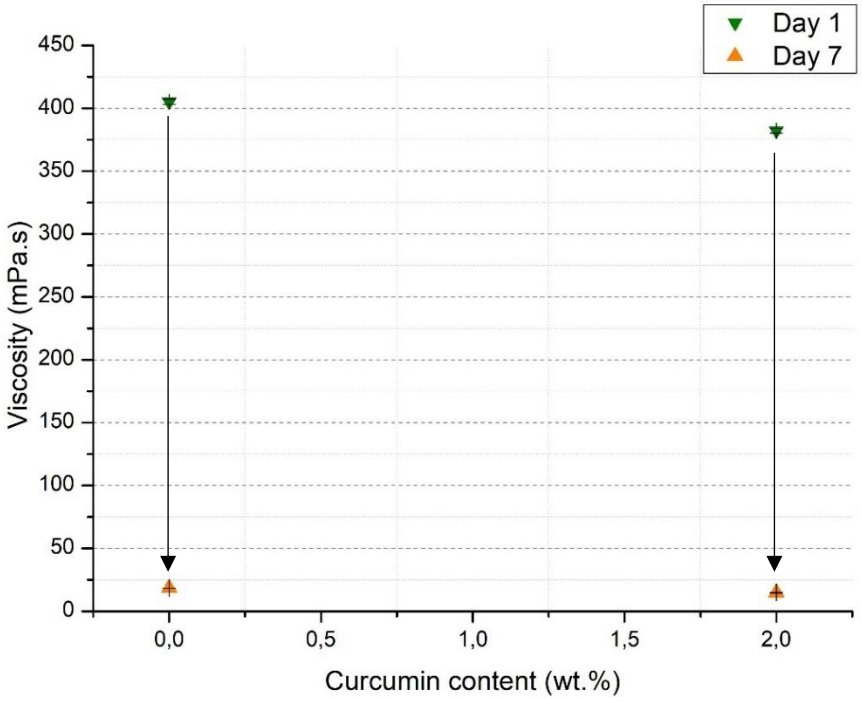

Figure 12: Viscosity of PCL and PCL/CUR-2 solutions as-prepared and after one week. Solutions after 1 day stirring (inverted green triangle) and 7 days stirring (orange triangle)

Viscosity measurements were also performed on every PCL solutions loaded with different percentages of aloe vera and curcumin. It was observed that the loading of curcumin generally decreased the solution viscosity and an increase of viscosity compared with neat PCL. In both solutions PCL/AV and PCL/CUR the viscosity measurements were above the minimum viscosity for electrospinability, 100 mPa.s[68]. These results can be seen in figure 13.

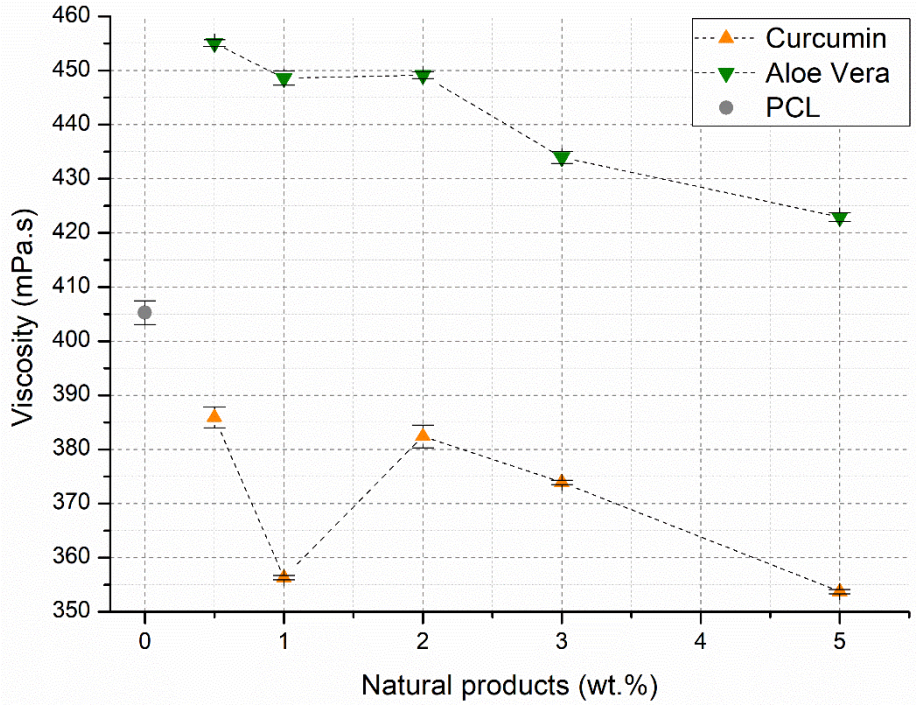

Figure 13: Viscosity measurements of PCL (grey circle) and PCL blends of AV (inverted green triangle) and CUR (orange triangle) with different percentages. (*p<0.05)

Conductivity

Conductivity of the solutions of PCL and PCL loaded with curcumin and aloe vera was measured. Compared with the value for the neat PCL solution (41.3 ± 4.1) µS/cm, a slight increase in the conductivity was confirmed for the solution loaded with curcumin (67.9 ± 4.5) µS/cm and a significant increase for the aloe vera loaded solution (462.3 ± 5.1) µS/cm.

According to the literature, loading ions to a solution may increase its electrical conductivity[69]. In this case, since the curcumin loaded solution was in an acid solution, and there is the presence of hydroxyl groups, the protonation of hydroxyl groups leads to an increase in conductivity as the content of curcumin increases. On the aloe vera, the same protonation happens on the sugars present. Aloe vera has several chemical elements such as Na, K, Ca, Mg, Mn, Cu, Zn, Cr, and Fe[42]. The presence of these chemical elements increases the electrical conductivity of the solution as the content of aloe vera is increased. Curcumin is an isolated compound, but aloe vera is an extract. It contains sugars, amino acids, chemical elements, and other compounds with similar groups and other chemical groups that could also protonate. Therefore,

the conductivity increase is higher in the solutions containing aloe vera than in the ones with added curcumin. The results are shown in figure 14.

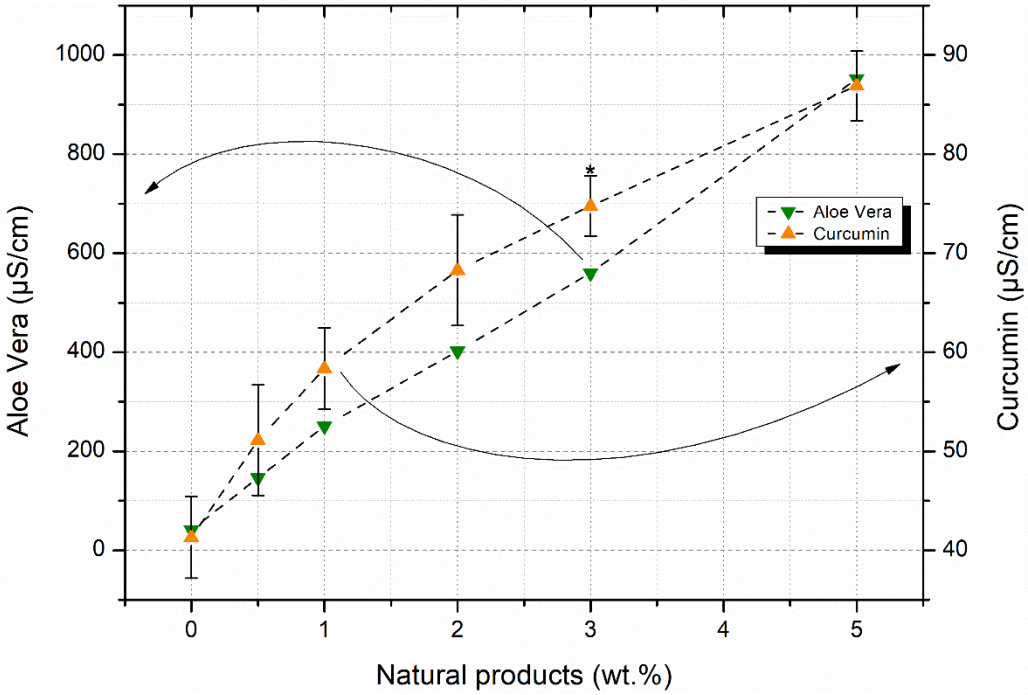

Figure 14: Conductivity measurements of solutions with different percentages of PCL loaded with aloe vera (left axis, inverted green triangle) and curcumin (right axis, orange triangle). (*p<0.05)

3.1.3. Electrospun membranes of PCL loaded with curcumin and aloe vera

Using the defined parameters (0.17 mL/h, 18 cm distance, 2000 rpm, 18kV), aloe vera and curcumin were loaded into the polymer's solutions with different mass percentages (0.5% to 5.0%) in the membrane. Fiber alignment and diameter were analyzed in every membrane through SEM observation.

Fiber alignment

Ten electrospun membranes of PCL loaded with different percentages of aloe vera (PCL/AV) (figure 15) and loaded with curcumin (PCL/CUR) (figure 16) were developed. The membranes were then observed by SEM and the diameter of fibers was analyzed through *ImageJ* and the alignment using the plugin "*OrientationJ*". This plugin permitted a visual observation of the orientation and a number to characterize

the coherency of the membranes. The higher percentage, the more aligned the fibers are.

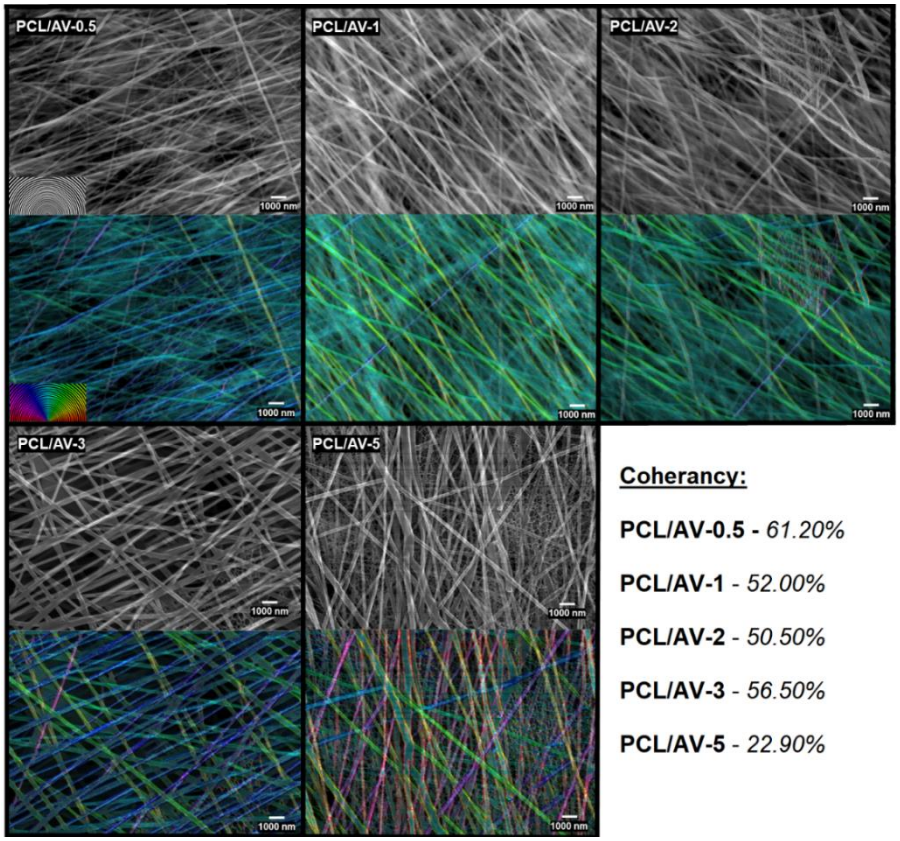

Figure 15: SEM image of PCL loaded with aloe vera at different percentages, a color image from SEM using *Orientation J* (below), and their coherency percentage.

Membranes of PCL loaded with aloe vera demonstrated a higher alignment (above 50% coherency) compared with the membranes loaded with curcumin (below 50% coherency). However, curcumin and aloe vera loading into the PCL membranes had produced a lower alignment than neat PCL (81.20% coherency). PCL/AV-5 had the lower fiber alignment among all the other membranes loaded with aloe vera. This could be explained by the appearance of a web-fiber-like between the fibers, also known as, nano-net, occupying most of the observed surface in this membrane, figure 17. But it was not the only membrane with these nano-nets PCL/AV-2, PCL/AV-3, and PCL/CUR-1 also exhibited these nanostructured (figure 19, around yellow squares). The formation of these nano-nets will be explained further in the thesis.

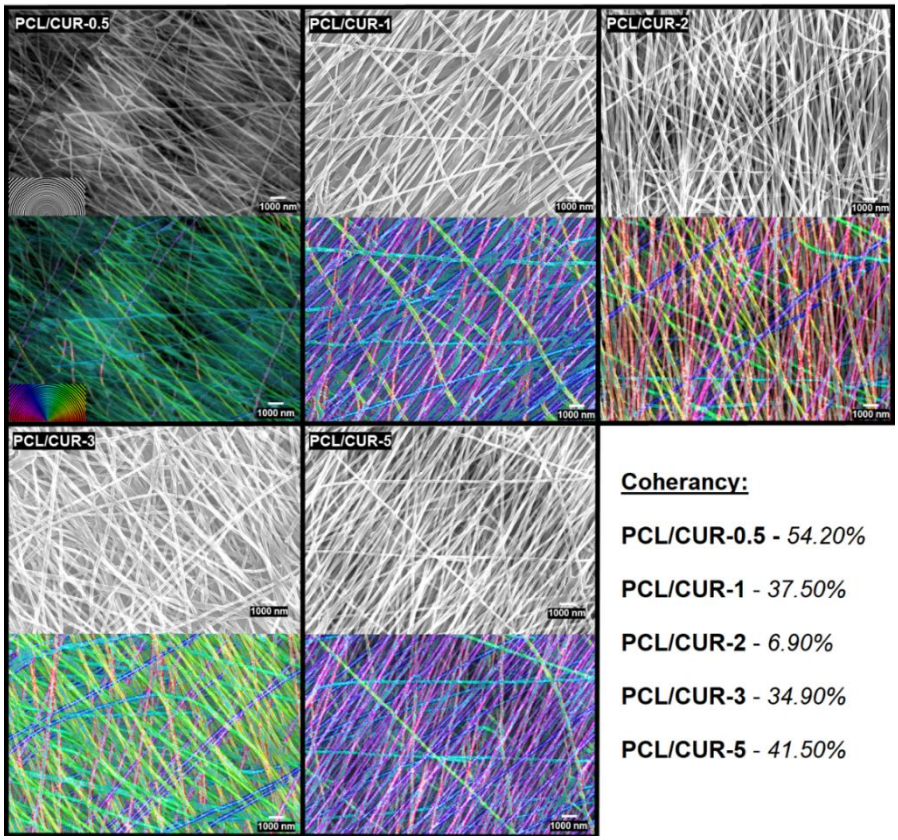

Figure 16: SEM image of PCL loaded with curcumin at different percentages, a color image from SEM using *Orientation J* (below), and their coherency percentage.

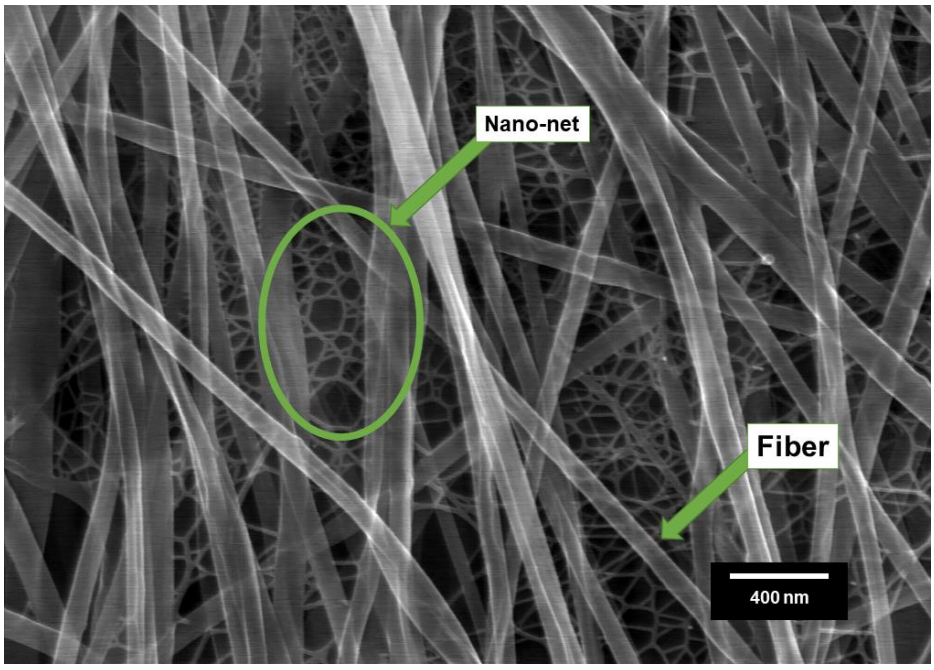

Figure 17: SEM image of PCL/AV-5 membrane showing the fiber on the green arrow, and around the circle the nano-net formation.

Fiber diameter

The results on fiber diameter analysis using ImageJ, demonstrated in table 8, showed that the fiber diameter of PCL membranes loaded with aloe vera had a similar fiber diameter to those of neat PCL (146.82 ± 53.38) nm. And, in the membranes that had a nano-net formation, the diameter of the supporting fiber was higher than those that did not have any, as observed when comparing PCL/AV-5 fiber diameter (183.36 ± 59.04) nm with PCL/AV-1 (157.72 ± 34.29) nm. Since the conductivity of the solution was much higher when loading aloe vera than neat PCL, fiber diameter usually decreases. Still, as it could be seen, that was not the case.

Membranes loaded with curcumin have demonstrated fiber diameters like those of neat PCL, except PCL/CUR-0.5, which had the lower fiber diameter of every membrane (119.55 ± 30.10) nm. Nano-net fiber diameter was also analyzed, and the range of these nets was from 26 nm to 42 nm (the results of fiber diameter and alignment in Table 8).

Table 8: Fiber diameter and coherency alignment for every electrospun membrane of PCL with the bioactive compound with different %w/w.

	Diameter (nm)		**Coherency**
	Fiber	*nano-net*	
PCL	146.82 ± 53.38	----	81.20%
PCL/AV-0.5	136.48 ± 29.13	----	61.20%
PCL/AV-1	157.72 ± 34.29	----	52.00%
PCL/AV-2	158.83 ± 39.43	26.30 ± 6.64	50.50%
PCL/AV-3	182.32 ± 44.94	42.28 ± 9.27	56.50%
PCL/AV-5	183.36 ± 59.04	31.58 ± 7.93	22.90%
PCL/CUR-0.5	119.55 ± 30.10	----	54.20%
PCL/CUR-1	167.06 ± 98.71	35.05 ± 7.61	37.50%
PCL/CUR-2	155.36 ± 42.60	----	6.90%
PCL/CUR-3	178.07 ± 42.28	----	34.90%
PCL/CUR-5	156.66 ± 29.96	----	41.50%

With the help of the boxplot (figure 18) and with the data of the diameters of each electrospun membrane (table 8), it is possible to observe that the range of diameters went from 120 nm to 184 nm, having in four membranes a net fiber diameter with the range 27 nm to 43 nm. This net was an interesting finding because it is composed of

diameters six times lower than the supporting fibers themselves. This process of webs formation is known nanofiber netting (NFN).

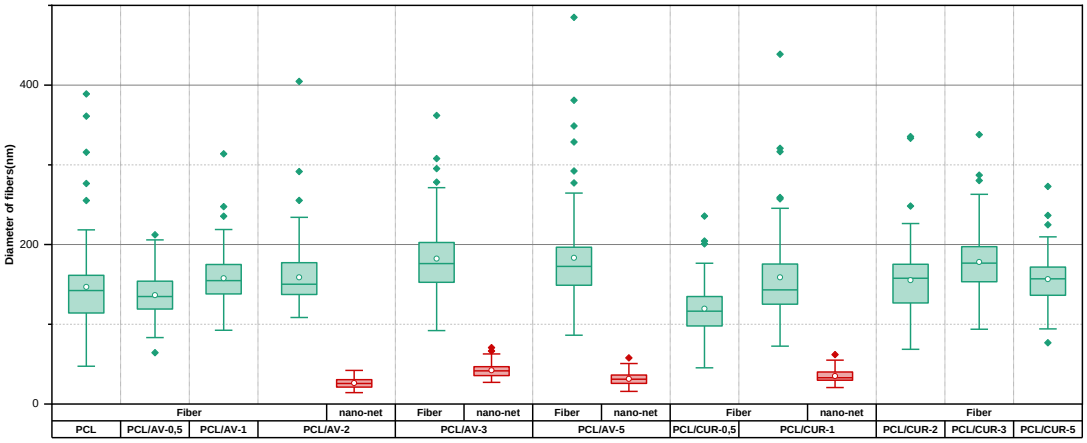

Figure 18: Boxplot of fiber diameters of electrospun membranes of PCL, PCL/AV, and PCL/CUR at different content percentages. Green boxes refer to diameters of the main membrane fibers and red boxes to nano-net fibers.

Nano-netting

The formation of nano-nets at different concentrations of aloe vera and curcumin in PCL, shown in figure 19 inside the yellow squares. It is reported in the literature for other polymeric formulations and associated with a technique known as nanofiber netting or electrospinning/netting (ESN).[81]

ESN was first found in 2004 and explained through a mechanism proposed in 2006 by Ding and co-workers[82], combining the conventional electrospinning process with electro-netting technology. This technology allows the formation of many net-like structured nanowires with small diameters (~20nm) distributed among conventional electrospun fibers.[58,83] NFN have been successfully processed by the ESN technique using synthetic and natural polymer solutions, thereby obtaining materials that overcome the properties of traditional nanofibers. Because of their small porosity, these web structure can be used in different applications, such as filters, sensors, and tissue engineering. Different polymer systems are known to produce NFN membranes, such as poly(acrylic acid) (PAA), poly(amide-6) (PA-6), poly(amide-66) (PA-66), PVA, Gel, chitosan, poly(urethane) (PU), and PCL.[82,84]

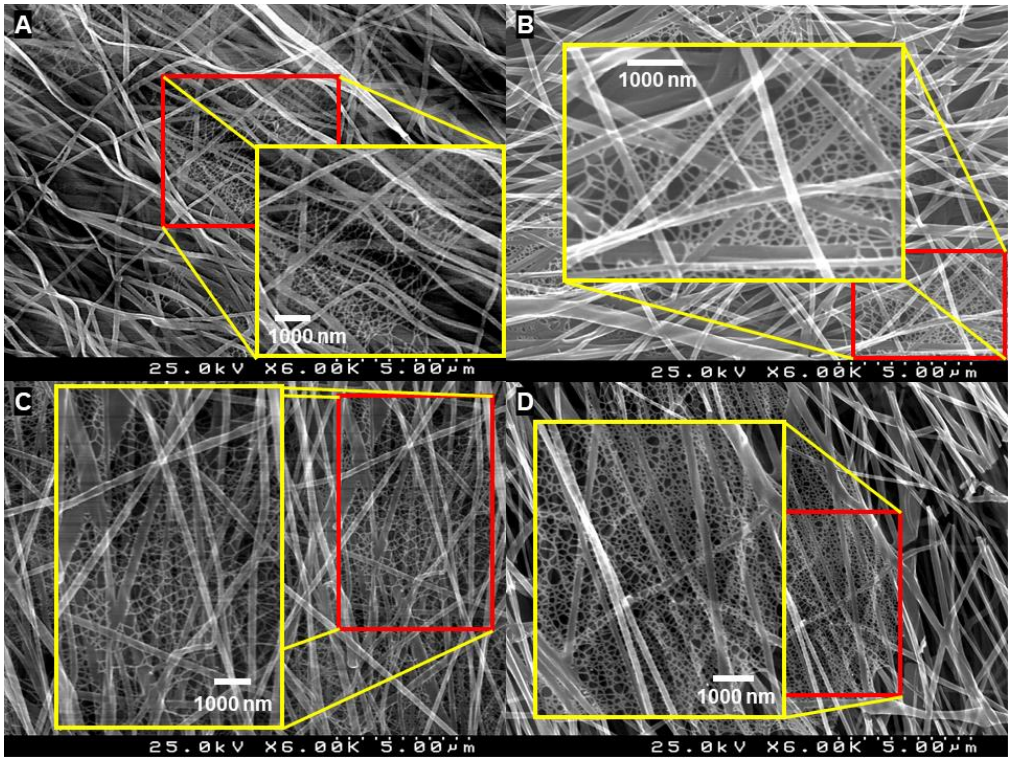

Figure 19: Electrospun nanofibers and nano-webs shown, where an approximation of the red square section can be seen inside the yellow squares to observe the nano-nets, (A) PCL/AV-2; (B) PCL/AV-3; (C) PCL/AV-5; (D) PCL/CUR-1.

Although this technique was found long ago, the formation mechanism has yet to be fully understood, and no consensus has been reached. Wang et al.[81] have extensively reviewed ESN, where the proposed mechanisms for the nano-nets formation can also be found. The phase separation of charged droplets generally produces Nano-nets formation. But different mechanisms suggest the formation of nano-nets:

Phase separation of charged droplets - is the general mechanism process. The rapid phase separation is induced from the deformation of charged droplets because of a high electric field force.

Formation of joints due to ions present in solution – where studies have shown that nano-net can be prepared by adding strong ionic salts[85]. When Ions are loaded to the electrospinning solution, they attached on the polymer chain cause a splitting of the nanofiber and the ions react and join together, creating the nano-net.

Intramolecular hydrogen bonding – that with high applied voltage the protonated amide group can connect with oxygen atom of PA-6 in the main fiber and oxygen

atom of an ionic molecule can create a hydrogen bond with the amide and oxygen of the main fiber as usual, both of which can interconnect and create the nano-fiber[86].

Sub-jets intertwining during jet flight – where some reports also indicate that while producing nanofibers on electrospinning, a main jet and sub-jets are formed simultaneously. It can cause a whipping or bending effect on the main jet during the jet flight but on the sub-jets. This whipping effect on the main jet and sub-jet a short contact time could have created the nano-nets once they are collected on the collector[87].

The NFN membranes favor the scaffold's cell proliferation and mechanical properties because the high porosity and low fibers diameter mimic the structure of collagen fibers within the ECM. There are only a few studies regarding the use of PCL for the formation of nano-nets. PCL has been blended with different products, such as Human Serum Albumin (HAS)[84,88], chitosan[22], wool keratin[89], Zein/Gum Arabic/*Calendula officinalis* extract[90], poly(ethylene glycol) (PEG)[91], and clusters of boron nitride nanotubes (BNNTs)[92]. All works have in common that the presence of nano-nets increased the biocompatibility, cell proliferation and attachment, and mechanical strength of the material.

In the present work, the formation of the nano-nets in the membranes of PCL/AV and PCL/CUR could be explained by the development of joints due to the ions present in the solution, in the case of aloe vera powder. However, this does not explain the nano-net formation for curcumin since the solution of curcumin is not so rich in ions. A study in the literature described that the use of formic acid to produce PVA membranes could act as a solvent and as a crosslinking agent contributing to the formation of the nano-nets.[93] Since formic acid was used as a solvent in the curcumin containing solution, it is likely to be this one the mechanism explaining the formation of nano-nets in the curcumin loaded membranes. Further studies need to be conducted to clarify this issue, testing, for example, other solvents and different polymer blends.

3.2. Physical chemical characterization of scaffolds

3.2.1. Attenuated Total Reflection – Fourier Transform Infra-red

The functional groups and chemical bonds of compounds incorporated into the nanofibers were analyzed using ATR-FIR. Figure 20 represents the ATR-FTIR spectra in transmittance of the various electrospun membranes and natural products. PCL spectrum showed characteristic peaks of $-CH_2$ (symmetric) and $-CH_2$ (asymmetric) vibrations at 2949-1868 cm^{-1} and a predominant peaking at 1722 cm^{-1} corresponding to ester stretching observed in all electrospun nanofibers membranes with PCL. The presence of hydroxyl group can be found at 3435 cm^{-1} on PCL membrane with AV and the AV isolated with a slight shift between those two. The PCL/AV spectrum peak at 3435 cm^{-1} ([94]) confirms that AV is incorporated on PCL/AV membrane. The stretching vibrations at 1515 cm^{-1} (C=C) in PCL/CUR and CUR correspond to the characteristic peaks of CUR.[95] Overall, the ATR-FTIR analysis demonstrated the presence of AV and CUR in the PCL membranes.

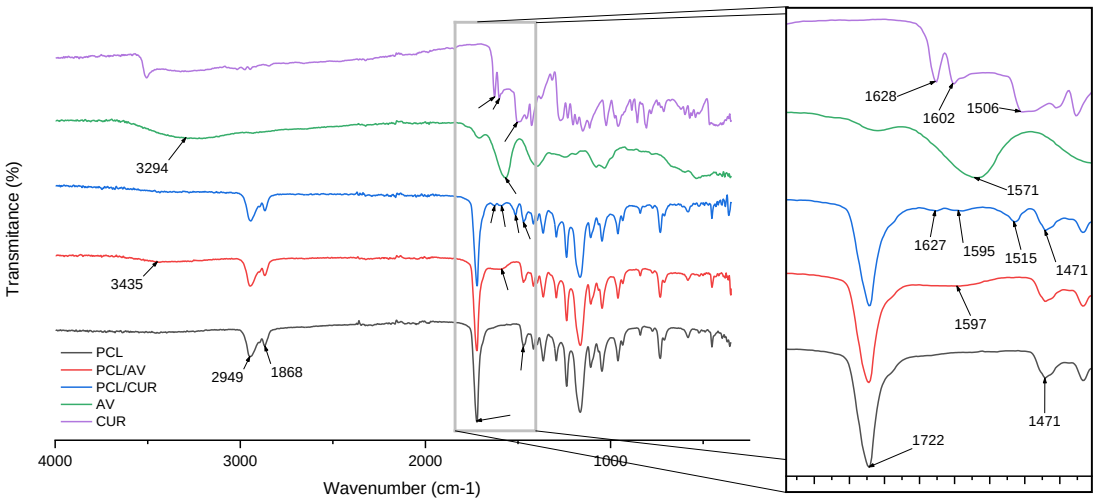

Figure 20: ATR-FTIR analysis of PCL, PCL/AV-5, and PCL/CUR-5 electrospun membranes and AV and CUR powder.

3.2.2. Wettability Tests

The hydrophobicity/hydrophilicity of a material can be evaluated using a wettability test. Contact angle analysis of a membrane is done to access the

biomaterial's surface and understand how it influences cell adhesion, cellular growth, and proliferation. The value of the water contact angle onto the material indicates the hydrophobicity/hydrophilicity of that material. If the contact angle is higher than 90º the material is hydrophobic, and for values lower than 90º the material is hydrophilic.[96]

The contact angle results obtained on the PCL membranes with the loading of aloe vera and curcumin are presented in figure 21. It shows that the contact angle decreased by loading the natural products, but the membranes are still hydrophobic because the values of contact angle are generally higher than 90º. It is possible to observe that with the increase of aloe vera and curcumin loading, the contact angle remains approximately constant as the weight percentage increases. The result of contact angle on neat PCL agrees with the value reported in the literature.[96]

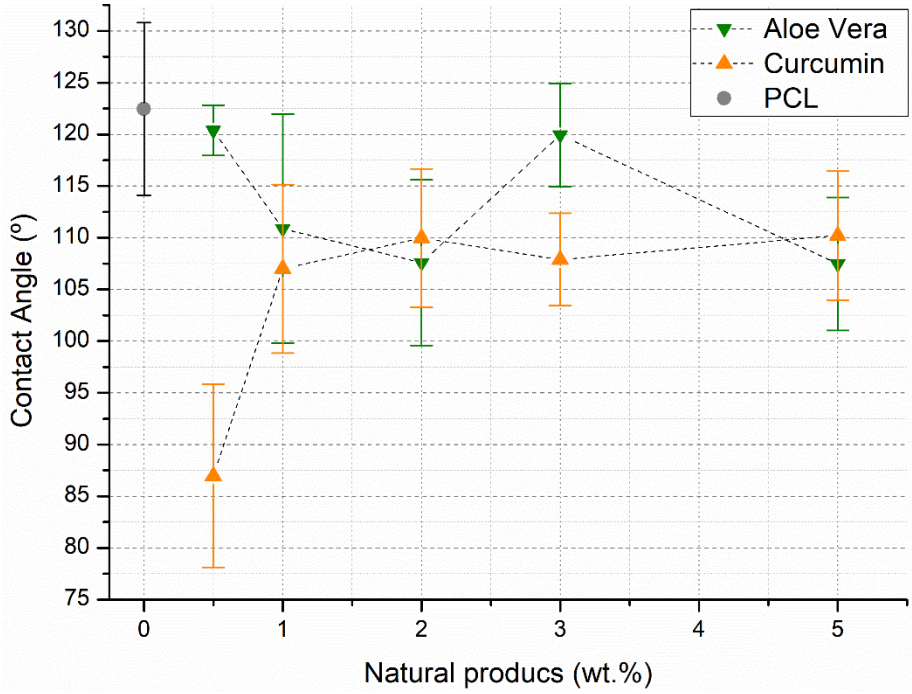

Figure 21: Contact angle analysis of water drop on the electrospun PCL membranes loaded with aloe vera (inverted green triangle) and with curcumin (orange triangle). (* $p<0.05$)

The results of the wettability test of the membranes loaded with aloe vera and curcumin demonstrated that the membranes are hydrophobic, and the loading of aloe vera and curcumin in different contents was not enough to change the hydrophobicity of membranes. This feature will produce a certain response from the biological environment. According to the literature, higher hydrophobicity usually leads to a high protein adsorption.[97]

3.3. Antibacterial activity assay of electrospun membranes

An antibacterial activity assay was performed on every electrospun membrane, with a neat PCL membrane as the control group since PCL has no antibacterial activity. The antibacterial effect can be confirmed by the appearance of a halo around the disks, which corresponds to the zone of inhibition. The higher the halo, the higher the antibacterial effect.[98] As shown in table 9, the protocol used for the bacterial tests indicated that no antibacterial activity was observed in any membranes with different percentages of curcumin and aloe vera.

Table 9: Tests results of antibacterial assay of PCL/CUR and PCL/AV samples with different wt.% against *E. Coli* (ATCC 25922) and *S. Aureus* (ATCC 29213) 24h incubation.

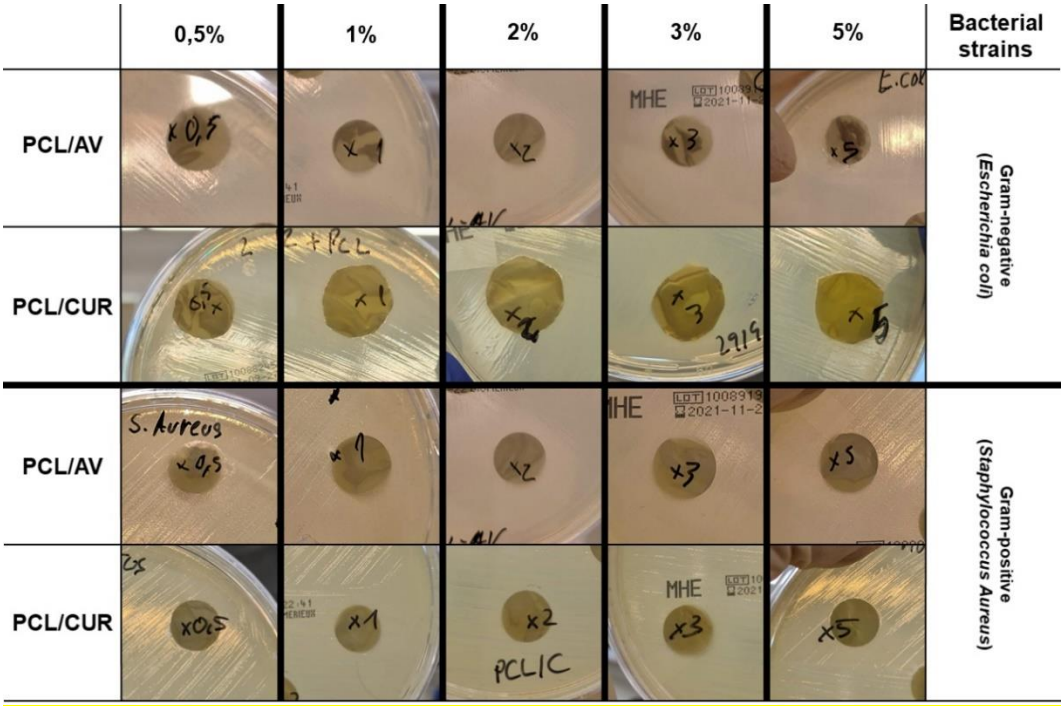

These results showed that the loading of curcumin and aloe vera powder doesn't interfere with bacterial growth, therefore not having any antibacterial effect. This result was not expected since it is known and reported in the literature that curcumin damages the cellular wall, and aloe vera blocks the bacterial adherence to the host epithelium leading to an antibacterial effect[52–54].

Further antibacterial tests need to be performed, and another control group should be considered. A suspension antibacterial method could have been used instead of the one followed in this work. The acid solvent used to dissolve PCL, curcumin, and aloe vera may have had affected the antibacterial activities of these compounds. This possibly needs to be explored in further work. Other controls, namely a solution of curcumin and a solution of aloe vera alone, could help the clarification of its antibacterial activity.

In the case of curcumin, one way to develop the antibacterial effect could be photodynamic therapy since curcumin is known to be a photosensitizer compound. This means that when irradiated with the proper wavelength, curcumin is activated and reacts to oxygen producing ROS, such as free radicals and singlet oxygen that have an antibacterial effect and at the same time are non-toxic to host cells. Previous studies have shown that a higher concentration of curcumin (75 μM) can produce enough ROS to have an antibacterial effect.[52,99] One other approach could be using microcapsules inserted onto the electrospun membrane since it is reported that when inserted curcumin into microcapsules, there is an antibacterial effect[29].

4. Conclusion and future approaches

This thesis had the objective to produce electrospun mats of PCL loaded with natural products, aloe vera and curcumin, to be applied as GTR membranes to treat periodontitis and stimulate periodontal tissue regeneration.

Membranes of PCL with different concentrations of aloe vera and curcumin were prepared using the electrospinning technique and green acids, such as acetic acid and formic acid, as solvents.

The conductivity of the solutions increased, either with the loading of aloe vera or with curcumin loading. Viscosity characterization of each solution before electrospinning showed that the loading of curcumin generally decreased the solution viscosity and the loading of aloe vera led to an increase on the viscosity (0.5% AV 455,1 ± 0.6 mPa.s) when compared to PCL (405,3 ± 2.2 mPa.s), and a lower viscosity when loaded with curcumin (0.5% CUR - 385.9 ± 1.9 mPa.s).

The loading of aloe vera and curcumin onto the electrospun membranes was confirmed using ATR-FTIR.

SEM analysis of the membranes presented bead-free continuous nanofibers in every membrane. Fibers alignment and diameters were measured through Image J tools. Electrospun nanofibers of PCL, PCL/AV, and PCL/CUR showed a range of diameters of 120-180 nm. In some membranes, PCL/AV-2, PCL/AV-3, PCL/AV-5, and PCL/CUR-1 the appearance of nano-net fibers was observed with fiber diameters ranging from 25-42 nm.

Contact angle analysis demonstrated that all the electrospun membranes, PCL, PCL/AV, and PCL/CUR are hydrophobic. The loading of aloe vera and curcumin did not change its surface hydrophobicity.

The antibacterial activity assays performed with all the electrospun membranes PCL, PCL/AV, and PCL/CUR detected no antibacterial activity in any of the membranes. In pursuit of the antibacterial effect of the loaded electrospun membranes, different experimental approaches should be performed to quantify antibacterial activity.

Overall, the electrospun membranes of PCL, PCL/AV, and PCL/CUR were successfully produced and showed promising results as a tissue engineering scaffold once they exhibited microstructural nanoscale features closely mimicking the ECM. The production of nano-nets between fibers should be further explored because its high surface area and nanostructure can extraordinarily benefit cellular regeneration.

4. Bibliography

1. Dr Poul Erik Petersen. Diet and Oral Health. *World Heal. Organ.* (2018).

2. Slots, J. Focal infection of periodontal origin. *Periodontol. 2000* **79**, 233–235 (2019).

3. Perillo, L., D'Apuzzo, F., Illario, M., Laino, L., Di Spigna, G., Lepore, M. Camerlingo, Carlo *et al.* Monitoring Biochemical and Structural Changes in Human Periodontal Ligaments during Orthodontic Treatment by Means of Micro-Raman Spectroscopy. *Sensors* **20**, 497 (2020).

4. Dr. Songa Vajra Madhuri. Membranes for Periodontal Regeneration. *Int. J. Pharm. Sci. Invent.* **5**, 19–24 (2016).

5. Piattelli, A., Scarano, A., Russo, P. & Matarasso, S. Evaluation of guided bone regeneration in rabbit tibia using bioresorbable and non-resorbable membranes. *Biomaterials* **17**, 791–796 (1996).

6. Haffajee, A. D. & Socransky, S. S. Microbial etiological agents of destructive periodontal diseases. *Periodontol. 2000* **5**, 78–111 (1994).

7. Abdelaziz, D., Hefnawy, A., Al-Wakeel, E., El-Fallal, A. & El-Sherbiny, I. M. New biodegradable nanoparticles-in-nanofibers based membranes for guided periodontal tissue and bone regeneration with enhanced antibacterial activity. *J. Adv. Res.* **28**, 51–62 (2021).

8. Rodriguez, IA., Selders, G. S., Fetz, A. E., Gehrmann C. J., Stein, S. H., Evensky, J. A., Green, M. S., Bowlin, G. L. Barrier membranes for dental applications: A review and sweet advancement in membrane developments. *Mouth and Teeth* **2**, 1–9 (2018).

9. Qasim, S. S. B., Baig, M. R., Matinlinna, J. P., Daood, U. & Al-Asfour, A. Highly Segregated Biocomposite Membrane as a Functionally Graded Template for Periodontal Tissue Regeneration. *Membranes (Basel).* **11**, 667 (2021).

10. Huang, Z., Feng, Q., Yu, B. & Li, S. Biomimetic properties of an injectable chitosan/nano-hydroxyapatite/collagen composite. *Mater. Sci. Eng. C* **31**, 683–687 (2011).

11. Tamburaci, S. & Tihminlioglu, F. Development of Si doped nano hydroxyapatite reinforced bilayer chitosan nanocomposite barrier membranes for guided bone regeneration. *Mater. Sci. Eng. C* **128**, 112298 (2021).

12. Ho, M., Claudia, J. C., Tai, W., Huang, K., Lai, C., Chang, C., Chang, Y., Wu, Y., Kuo, M. Y., Chang, P. The treatment response of barrier membrane with amoxicillin-loaded nanofibers in experimental periodontitis. *J. Periodontol.* **92**, 886–895 (2021).

13. Ferreira, A. M., Gentile, P., Chiono, V. & Ciardelli, G. Collagen for bone tissue regeneration. *Acta Biomater.* **8**, 3191–3200 (2012).

14. Peng, W., Ren, S., Zhang, Y., Fan, R., Zhou, Y., Li, L., Xu, X., Xu, Y. MgO Nanoparticles-Incorporated PCL/Gelatin-Derived Coaxial Electrospinning Nanocellulose Membranes for Periodontal Tissue Regeneration. *Front. Bioeng. Biotechnol.* **9**, 1–13 (2021).

15. Rezk, A. I., Mousa, H. M., Lee, J., Park, C. H. & Kim, C. S. Composite PCL/HA/simvastatin electrospun nanofiber coating on biodegradable Mg alloy for orthopedic implant application. *J. Coatings Technol. Res.* **16**, 477–489 (2019).

16. Ezhilarasu, H., Ramalingam, R., Dhand, C., Lakshminarayanan, R., Sadiq, A., Gandhimathi, C., Ramakrishna, S., Bay, B. H., Venugopal, J. R., Srinivasan, D. K. Biocompatible Aloe vera and Tetracycline Hydrochloride Loaded Hybrid Nanofibrous Scaffolds for Skin Tissue Engineering. *Int. J. Mol. Sci.* **20**, 5174 (2019).

17. Bartnikowski, M., Dargaville, T. R., Ivanovski, S. & Hutmacher, D. W. Degradation mechanisms of polycaprolactone in the context of chemistry, geometry and environment. *Prog. Polym. Sci.* **96**, 1–20 (2019).

18. Rydz, J., Sikorska, W., Kyulavska, M. & Christova, D. Polyester-Based (Bio)degradable Polymers as Environmentally Friendly Materials for Sustainable Development. *Int. J. Mol. Sci.* **16**, 564–596 (2014).

19. Bongiovanni Abel, S., Liverani, L., Boccaccini, A. R. & Abraham, G. A. Effect of benign solvents composition on poly(ε-caprolactone) electrospun fiber properties. *Mater. Lett.* **245**, 86–89 (2019).

20. Sharma, D., Saha, D. & Satapathy, B. K. Structurally optimized suture resistant polylactic acid (PLA)/poly (ϵ-caprolactone) (PCL) blend based engineered nanofibrous mats. *J. Mech. Behav. Biomed. Mater.* **116**, 104331 (2021).

21. Shabannejad, M., Nourbakhsh, M. S., Salati, A. & Bahrami, Z. Fabrication and Characterization of Electrospun Scaffold Based on Polycaprolactone-Aloe vera and Polyvinyl Alcohol for Skin Tissue Engineering. *Fibers Polym.* **21**, 1694–1703 (2020).

22. Habibizadeh, M. Nadri, S., Fattahi, A., Rostamizadeh, K., Mohammadi, P., Andalib, S., Hamidi, M., Forouzideh, N. Surface modification of neurotrophin-3 loaded PCL/chitosan nanofiber/net by alginate hydrogel microlayer for enhanced biocompatibility in neural tissue engineering. *J. Biomed. Mater. Res. Part A* **109**, 2237–2254 (2021).

23. Thompson, Z., Rahman, S., Yarmolenko, S., Sankar, J., Kumar, D., Bhattarai, N. Fabrication and Characterization of Magnesium Ferrite-Based PCL/Aloe Vera Nanofibers. *Materials (Basel).* **10**, 937 (2017).

24. Kim, J. H., Choung, P., Kim, I. Y., Lim, K. T., Son, H. M., Choung, Y., Cho, C., Chung, J. H. Electrospun nanofibers composed of poly(ε-caprolactone) and polyethylenimine for tissue engineering applications. *Mater. Sci. Eng. C* **29**, 1725–1731 (2009).

25. Rahman, S., Carter, P. & Bhattarai, N. Aloe Vera for Tissue Engineering Applications. *J. Funct. Biomater.* **8**, 6 (2017).

26. Pachuau, L., Laldinchhana, Roy, P., Zothantluanga, J. H., Ray, S., Das, S. Encapsulation of Bioactive Compound and Its Therapeutic Potential. in *Bioactive Natural Products for Pharmaceutical Applications* (eds. Pal, D. & Nayak, A. K.) 687–714 (Springer, 2021).

27. Ferreira, V. H., Nazli, A., Dizzell, S. E., Mueller, K. & Kaushic, C. The Anti-Inflammatory Activity of Curcumin Protects the Genital Mucosal Epithelial Barrier from Disruption and Blocks Replication of HIV-1 and HSV-2. *PLoS One* **10**, e0124903 (2015).

28. Bourne, K. Z., Bourne, N., Reising, S. F. & Stanberry, L. R. Plant products as topical microbicide candidates : assessment of in vitro and in vivo activity against herpes simplex virus type 2. *Antiviral Res.* **42**, 219–226 (1999).

29. Wang, Y., Lu, Z., Wu, H. & Lv, F. Study on the antibiotic activity of microcapsule curcumin against foodborne pathogens. *Int. J. Food Microbiol.* **136**, 71–74 (2009).

30. Celik, H., Aydin, T., Solak, K., Khalid, S. & Farooqi, A. A. Curcumin on the “flying carpets” to modulate different signal transduction cascades in cancers: Next-

generation approach to bridge translational gaps. *J. Cell. Biochem.* **119**, 4293–4303 (2018).

31. Rathinavel, S., Korrapati, P. S., Kalaiselvi, P. & Dharmalingam, S. Mesoporous silica incorporated PCL/Curcumin nanofiber for wound healing application. *Eur. J. Pharm. Sci.* **167**, 106021 (2021).

32. Mashayekhi, S., Rasoulpoor, S., Shabani, S., Esmaeilizadeh, N., Serati-Nouri, H., Sheervalilou, R., Pilehvar-Soltanahmadi, Y. Curcumin-loaded mesoporous silica nanoparticles/nanofiber composites for supporting long-term proliferation and stemness preservation of adipose-derived stem cells. *Int. J. Pharm.* **587**, 119656 (2020).

33. Chattopadhyay, I., Biswas, K., Bandyopadhyay, U. & Banerjee, R. K. Turmeric and Curcumin: Biological actions and medicinal applications. *Curr. Sci.* **87**, 1476–1479 (2004).

34. Anand, P., Kunnumakkara, A. B., Newman, R. A. & Aggarwal, B. B. Bioavailability of Curcumin: Problems and Promises. *Mol. Pharm.* **4**, 807–818 (2007).

35. Bulbul, Y. E., Okur, M., Demirtas-Korkmaz, F. & Dilsiz, N. Development of PCL/PEO electrospun fibrous membranes blended with silane-modified halloysite nanotube as a curcumin release system. *Appl. Clay Sci.* **186**, 105430 (2020).

36. Silva, T. T., Cesar, G. B., Francisco, C. P., Mossini, G. G., Hoshino, L. V. C., Sato, F., Radovanovic, E., Agostini, D. L. S., Caetano, W., Hernandes, L., Matioli, G. Electrospun curcumin/polycaprolactone/copolymer F-108 fibers as a new therapy for wound healing. *J. Appl. Polym. Sci.* **137**, 48415 (2020).

37. Balashanmugam, P., Sucharithra, G., Mary, S. A. & Selvi, A. T. Efficacy of biopolymeric PVA-AuNPs and PCL-Curcumin loaded electrospun nanofibers and their anticancer activity against A431 skin cancer cell line. *Mater. Today Commun.* **25**, 101276 (2020).

38. Sadeghianmaryan, A., Yazdanpanah, Z., Soltani, Y. A., Sardroud, H. A., Nasirtabrizi, M. H., Chen, X. Curcumin-loaded electrospun polycaprolactone/montmorillonite nanocomposite: wound dressing application with anti-bacterial and low cell toxicity properties. *J. Biomater. Sci. Polym. Ed.* **31**, 169–187 (2020).

39. Zahiri, M., Khanmohammadi, M., Goodarzi, A., Ababzadeh, S., Farahani, M. S.,

Mohandesnezhad, S., Bahrami, N., Nabipour, I., Ai, J. Encapsulation of curcumin loaded chitosan nanoparticle within poly (ε-caprolactone) and gelatin fiber mat for wound healing and layered dermal reconstitution. *Int. J. Biol. Macromol.* **153**, 1241–1250 (2020).

40. Maan, A. A., Nazir, A., Khan, M. I., Ahmad, T., Zia, R., Murid, M., Abrar, M. The therapeutic properties and applications of Aloe vera : A review. *J. Herb. Med.* **12**, 1–10 (2018).

41. Bozzi, A., Perrin, C., Austin, S. & Arce Vera, F. Quality and authenticity of commercial aloe vera gel powders. *Food Chem.* **103**, 22–30 (2007).

42. Raghuvanshi, M., Rajesh, E., Sinha, S. & Babu, N. A. Aloevera: The Miracle Plant and Its uses in Dentistry – A Review. *Indian J. Forensic Med. Toxicol.* **14**, 1226–1229 (2020).

43. Hamman, J. H. Composition and Applications of Aloe vera Leaf Gel. *Molecules* **13**, 1599–1616 (2008).

44. Misir, J., H. Brishti, F. & M. Hoque, M. *Aloe vera* gel as a Novel Edible Coating for Fresh Fruits: A Review. *Am. J. Food Sci. Technol.* **2**, 93–97 (2014).

45. Boudreau, M. D., Beland, F. A. An Evaluation of the Biological and Toxicological Properties of Aloe Barbadensis (Miller), Aloe Vera. *J. Environ. Sci. Heal. Part C* **24**, 103–154 (2006).

46. Lima, L. L., Bierhalz, A. C. K. & Moraes, Â. M. Influence of the chemical composition and structure design of electrospun matrices on the release kinetics of Aloe vera extract rich in aloin. *Polym. Degrad. Stab.* **179**, 109233 (2020).

47. Baghersad, S., Hajir Bahrami, S., Mohammadi, M. R., Mojtahedi, M. R. M. & Milan, P. B. Development of biodegradable electrospun gelatin/aloe-vera/poly(ε-caprolactone) hybrid nanofibrous scaffold for application as skin substitutes. *Mater. Sci. Eng. C* **93**, 367–379 (2018).

48. Isola, G., Polizzi, A., Santonocito, S., Dalessandri, D., Migliorati, M., Indelicato, F. New Frontiers on Adjuvants Drug Strategies and Treatments in Periodontitis. *Sci. Pharm.* **89**, 46 (2021).

49. Zaatout, N. Presence of non-oral bacteria in the oral cavity. *Arch. Microbiol.* **203**, 2747–2760 (2021).

50. Socransky, S. S. Microbiology of Periodontal Disease - Present Status and Future Considerations. *J. Periodontol.* **48**, 497–504 (1977).

51. Cabeen, M. T. & Jacobs-Wagner, C. Bacterial cell shape. *Nat. Rev. Microbiol.* **3**, 601–610 (2005).

52. Abd El-Hack, M. E., El-Saadony, M. T., Swelum, A. A., Arif, M., Abo Ghanima, M. M., Shukry, M., Noreldin, A., Taha, A. E., El-Tarabily, K. A. Curcumin, the active substance of turmeric: its effects on health and ways to improve its bioavailability. *J. Sci. Food Agric.* **101**, 5747–5762 (2021).

53. Sierra-García, G. D., Castro-Ríos, R., González-Horta, A., Lara-Arias, J. & Chávez-Montes, A. Acemannan, an Extracted Polysaccharide from Aloe vera : A Literature Review. *Nat. Prod. Commun.* **9**, 1934578X1400900 (2014).

54. Yun, D. G. & Lee, D. G. Antibacterial activity of curcumin via apoptosis-like response in Escherichia coli. *Appl. Microbiol. Biotechnol.* **100**, 5505–5514 (2016).

55. Baumgarten, P. K. Electrostatic spinning of acrylic microfibers. *J. Colloid Interface Sci.* **36**, 71–79 (1971).

56. Formhals, A. Process and apparatus for preparing artificial threads. (1934).

57. Unnithan, A. R., Arathyram, R. S. & Kim, C. S. Electrospinning of Polymers for Tissue Engineering. in *Nanotechnology Applications for Tissue Engineering* 45–55 (Elsevier, 2015).

58. Massaglia, G., Chiodoni, A., Salvador, G. P., Delmondo, L., Muñoz-Tabares, J. A., Bocchini, S., Sacco, A., Bianco, S., Saracco, G., Quaglio, M. Defining the role of nanonetting in the electrical behaviour of composite nanofiber/nets. *RSC Adv.* **7**, 38812–38818 (2017).

59. Taylor, G. & Dyke, M. D. Van. Electrically driven jets. *Proc. Roy. Soc. Lond. A* **313**, 453–475 (1969).

60. Chew, S., Wen, Y., Dzenis, Y. & Leong, K. The Role of Electrospinning in the Emerging Field of Nanomedicine. *Curr. Pharm. Des.* **12**, 4751–4770 (2006).

61. Bhardwaj, N. & Kundu, S. C. Electrospinning: A fascinating fiber fabrication technique. *Biotechnol. Adv.* **28**, 325–347 (2010).

62. Yarin, A. L., Koombhongse, S. & Reneker, D. H. Taylor cone and jetting from liquid

droplets in electrospinning of nanofibers. *J. Appl. Phys.* **90**, 4836–4846 (2001).

63. Deitzel, J. M., Kleinmeyer, J., Harris, D. & Beck Tan, N. C. The effect of processing variables on the morphology of electrospun nanofibers and textiles. *Polymer (Guildf).* **42**, 261–272 (2001).

64. Norman, J. J. & Desai, T. A. Methods for Fabrication of Nanoscale Topography for Tissue Engineering Scaffolds. *Ann. Biomed. Eng.* **34**, 89–101 (2006).

65. Prabhakaran, M. P., Ghasemi-Mobarakeh, L. & Ramakrishna, S. Electrospun Composite Nanofibers for Tissue Regeneration. *J. Nanosci. Nanotechnol.* **11**, 3039–3057 (2011).

66. Doshi, J. & Reneker, D. . H. Electrospinning process and applications of electrospun fibers. in *Journal of Electrostatics* vol. 35 151–160 (Elsevier, 1995).

67. Zeng, J., Haoqing, H., Schaper, A., Wendorff, J. H. & Greiner, A. Poly-L-lactide nanofibers by electrospinning – Influence of solution viscosity and electrical conductivity on fiber diameter and fiber morphology. *e-Polymers* **3**, 1–9 (2003).

68. Fong, H., Chun, I. & Reneker, D. H. Beaded nanofibers formed during electrospinning. *Polymer (Guildf).* **40**, 4585–4592 (1999).

69. Ghaderpour, A., Hoseinkhani, Z., Yarani, R., Mohammadiani, S., Amiri, F., Mansouri, K. Altering the characterization of nanofibers by changing the electrospinning parameters and their application in tissue engineering, drug delivery, and gene delivery systems. *Polym. Adv. Technol.* **32**, 1924–1950 (2021).

70. Yuan, X., Zhang, Y., Dong, C. & Sheng, J. Morphology of ultrafine polysulfone fibers prepared by electrospinning. *Polym. Int.* **53**, 1704–1710 (2004).

71. Kumbar, S., Nukavarapu, S. P., James, R., Hogan, M. V. & Laurencin, C. T. Recent Patents on Electrospun Biomedical Nanostructures: An Overview. *Recent Patents Biomed. Eng.* **1**, 68–78 (2008).

72. Geng, X., Kwon, O., Jang, J. Electrospinning of chitosan dissolved in concentrated acetic acid solution. *Biomaterials* **26**, 5427–5432 (2005).

73. Fahmy, A., Zaid, H. & Ibrahim, M. Optimizing the electrospun parameters which affect the preparation of nanofibers. *Biointerface Res. Appl. Chem.* **9**, 4463–4473 (2019).

74. Capello, C., Fischer, U. & Hungerbühler, K. What is a green solvent? A

comprehensive framework for the environmental assessment of solvents. *Green Chem.* **9**, 927 (2007).

75. Chen, S., Galusková, D., Kaňková, H., Zheng, K., Michálek, M., Liverani, L., Galusek, D., Boccaccini, A. R. Electrospun PCL Fiber Mats Incorporating Multi-Targeted B and Co Co-Doped Bioactive Glass Nanoparticles for Angiogenesis. *Materials (Basel).* **13**, 4010 (2020).

76. Luo, C. J., Stride, E. & Edirisinghe, M. Mapping the Influence of Solubility and Dielectric Constant on Electrospinning Polycaprolactone Solutions. *Macromolecules* **45**, 4669–4680 (2012).

77. Basso, B. Fabricação de membranas de policaprolactona por electrospinning para medicina regenerativa. *Diss. Mestr. FEUP* (2019).

78. O'Neil, M. The Merck Index - An Encyclopedia of Chemicals, Drugs, and Biologicals. *R. Soc. Chem.* 474 (2013).

79. Püspöki, Z., Storath, M., Sage, D. & Unser, M. Transforms and Operators for Directional Bioimage Analysis: A Survey. in *Advances in Anatomy Embryology and Cell Biology* vol. 219 69–93 (2016).

80. Ghobeira, R., Asadian, M., Vercruysse, C., Declercq, H., De Geyter, N., Morent, R. Wide-ranging diameter scale of random and highly aligned PCL fibers electrospun using controlled working parameters. *Polymer (Guildf).* **157**, 19–31 (2018).

81. Wang, X., Ding, B., Sun, G., Wang, M. & Yu, J. Electro-spinning/netting: A strategy for the fabrication of three-dimensional polymer nano-fiber/nets. *Prog. Mater. Sci.* **58**, 1173–1243 (2013).

82. Ding, B., Li, C., Miyauchi, Y., Kuwaki, O. & Shiratori, S. Formation of novel 2D polymer nanowebs via electrospinning. *Nanotechnology* **17**, 3685–3691 (2006).

83. Wang, X., Ding, B., Yu, J., Si, Y., Yang, S., Sun, G. Electro-netting: Fabrication of two-dimensional nano-nets for highly sensitive trimethylamine sensing. *Nanoscale* **3**, 911–915 (2011).

84. Tiwari, A. P., Joshi, M. K., Park, C. H. & Kim, C. S. Nano-Nets Covered Composite Nanofibers with Enhanced Biocompatibility and Mechanical Properties for Bone Tissue Engineering. *J. Nanosci. Nanotechnol.* **18**, 529–537 (2018).

85. Barakat, N. A. M., Kanjwal, M. A., Sheikh, F. A. & Kim, H. Y. Spider-net within the

N6, PVA and PU electrospun nanofiber mats using salt addition: Novel strategy in the electrospinning process. *Polymer (Guildf).* **50**, 4389–4396 (2009).

86. Pant, H. R., Bajgai, M. P., Nam, K. T., Chu, K. H., Park, S., Kim, H. Y. Formation of electrospun nylon-6/methoxy poly(ethylene glycol) oligomer spider-wave nanofibers. *Mater. Lett.* **64**, 2087–2090 (2010).

87. Tsou, S.-Y., Lin, H.-S. & Wang, C. Studies on the electrospun Nylon 6 nanofibers from polyelectrolyte solutions: 1. Effects of solution concentration and temperature. *Polymer (Guildf).* **52**, 3127–3136 (2011).

88. Tiwari, A. P. *et al.* Bimodal fibrous structures for tissue engineering: Fabrication, characterization and in vitro biocompatibility. *J. Colloid Interface Sci.* **476**, 29–34 (2016).

89. Zhu, H., Li, R., Wu, X., Chen, K. & Che, J. Controllable fabrication and characterization of hydrophilic PCL/wool keratin nanonets by electronetting. *Eur. Polym. J.* **86**, 154–161 (2017).

90. Pedram Rad, Z., Mokhtari, J. & Abbasi, M. Biopolymer based three-dimensional biomimetic micro/nanofibers scaffolds with porous structures via tailored charge repulsions for skin tissue regeneration. *Polym. Adv. Technol.* **32**, 3535–3548 (2021).

91. Tiwari, A. P., Joshi, M. K., Lee, J., Maharjan, B., Ko, S. W., Park, C. H., Kim, C. S. Heterogeneous electrospun polycaprolactone/polyethylene glycol membranes with improved wettability, biocompatibility, and mineralization. *Colloids Surfaces A Physicochem. Eng. Asp.* **520**, 105–113 (2017).

92. Khalili, N. P., Moradi, R., Kavehpour, P., Islamzada, F. & Abdullayev, Y. Fabrication and biocompatibility of BNNT supramolecular complexes and PCL/BNNTs nanofibers. *Mater. Today Proc.* **42**, 1570–1578 (2021).

93. Wang, N., Si, Y., Yu, J., Fong, H. & Ding, B. Nano-fiber/net structured PVA membrane: Effects of formic acid as solvent and crosslinking agent on solution properties and membrane morphological structures. *Mater. Des.* **120**, 135–143 (2017).

94. Karuppuswamy, P., Venugopal, J. R., Navaneethan, B., Laiva, A. L., Sridhar, S., Ramakrishna, S. Functionalized hybrid nanofibers to mimic native ECM for tissue engineering applications. *Appl. Surf. Sci.* **322**, 162–168 (2014).

95. Mai, T. T. T., Nguyen, T. T. T., Le, Q. D., Nguyen, T. G., Ba, T. C., Nguyen, H. B., Phan, T. B. H., Tran, D. L., Nguyen, X. P., Park, J. S. A novel nanofiber Cur-loaded polylactic acid constructed by electrospinning. *Adv. Nat. Sci. Nanosci. Nanotechnol.* **3**, 025014 (2012).

96. Shalumon, K. T., Anulekha, K.H., Chennazhi, K.P., Tamura, H., Nair, S.V., Jayakumar, R. Fabrication of chitosan/poly(caprolactone) nanofibrous scaffold for bone and skin tissue engineering. *Int. J. Biol. Macromol.* **48**, 571–576 (2011).

97. Ogueri, K. S., Jafari, T., Escobar Ivirico, J. L. & Laurencin, C. T. Polymeric Biomaterials for Scaffold-Based Bone Regenerative Engineering. *Regen. Eng. Transl. Med.* **5**, 128–154 (2019).

98. Marques, C. F., Perera, F. H., Marote, A., Ferreira, S., Vieira, S. I., Olhero, S., Miranda, P., Ferreira, J. M. F. Biphasic calcium phosphate scaffolds fabricated by direct write assembly: Mechanical, anti-microbial and osteoblastic properties. *J. Eur. Ceram. Soc.* **37**, 359–368 (2017).

99. Paschoal, M. A., Tonon, C. C., Spolidório, D. M. P., Bagnato, V. S., Giusti, J. S. M., Santos-Pinto, L. Photodynamic potential of curcumin and blue LED against Streptococcus mutans in a planktonic culture. *Photodiagnosis Photodyn. Ther.* **10**, 313–319 (2013).

5. Appendix

5.1. Flow rate correction

A timer was counting from the beginning of the electrospinning until the end. The volume consumed in the syringe was calculated using the height of solution consumed in the syringe to measure the flow rate of the equipment, Q.

The electrospinning trial took 6 hours and 40 minutes to conclude. Time, T = 6.67 hours. The diameter, d, of the syringe used (6 mL) is 1.214 cm. The height consumed on the syringe, 0.84 cm. Q is the flow rate.

$$Q = \frac{V_{syringe}}{T} = \frac{\pi * \left(r_{syringe}\right)^2 * h}{T} = \frac{\pi * 0.607^2 * 0.84}{6.67} = 0.145\ mL/h$$

Using this value is possible to extrapolate the rest of the results since the flow rate set on this trial ($Q_{Equipment}$) was 0.4 mL/h and the real flow rate (Q_{Real}) was 0.145 mL/h. Using this extrapolation, the equation calculated is $Q_{Real} = 0.3625 * Q_{Equipment}$.

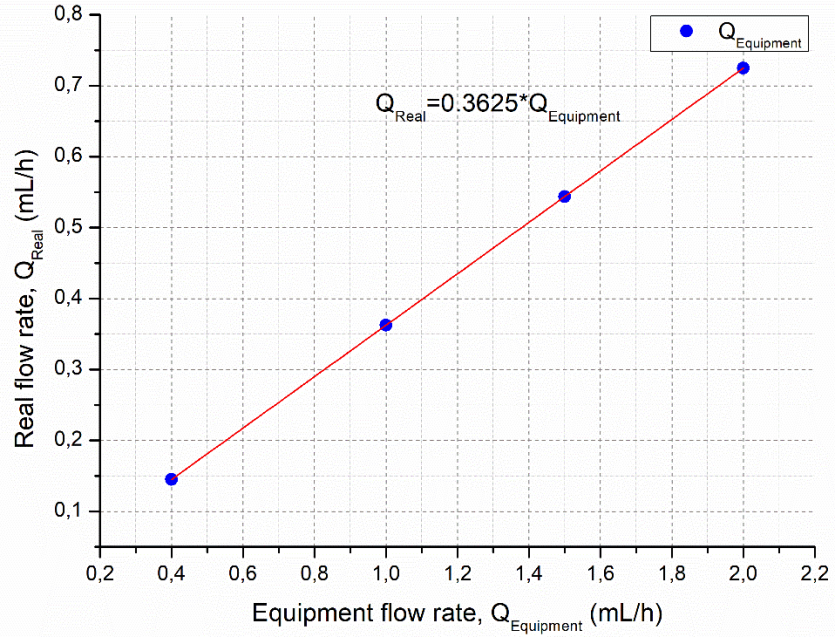

Figure 22: Correlation graph between the flow rate of the equipment against the real flow rate using a 6mL syringe and the linear correlation.